Studies on DNA methylation changes in canine malignant melanoma

(犬の悪性黒色腫における
DNA メチル化の変化に関する研究)

Teita Ishizaki

Table of Contents

Chapter 2

Long interspersed nucleotide element-1 hypomethylation in canine malignant mucosal melanoma

Chapter 3

Differences in DNA methylation status between epithelial and mesenchymal phenotypes in canine malignant melanoma

ABBREVIATIONS

CGIs	CpG islands
DAB	3,3'Diaminobenzidine
DMC	differentially methylated CpG sites
DREAM	Digital Restriction Enzyme Analysis of Methylation
LINE-1	Long Interspersed Nucleotide Element-1
MSI	microsatellite instability
NCGIs	non-CpG islands
NGS	Next-generation sequencing
PBS	phosphatase-buffered saline
TILs	tumor-infiltrating lymphocytes

Notes

Contents of the present thesis were published in the following articles.

1. Ishizaki T, Yamazaki J, Meagawa S, Yokoyama N, Aoshima K, Takiguchi M, Kimura T. 2020. Long interspersed nucleotide element-1 hypomethylation in canine malignant mucosal melanoma. Vet Comp Oncol. 18(4), 854-860.

2. Ishizaki T, Yamazaki J, Jelinek J, Aoshima K, Kimura T. 2020. Genome-wide DNA methylation analysis identifies promoter hypermethylation in canine malignant melanoma. Res Vet Sci.132, 521-526. doi: 10.1016/j.rvsc.2020.08.006. Epub

General Introduction

Canine malignant melanoma is one of the common cancers, accounting for 7% of all malignant tumors. They are highly aggressive and metastatic causing poor prognosis. While human malignant melanoma most commonly occurs in the skin, the most frequent location of canine malignant melanoma is the oral cavity including gingiva with less predominantly lingual, buccal, pharyngeal, tonsillar, and palatine epithelium [1]. Oral melanomas derive from neural crest cells that reside within the oral mucosal epithelium. Pathologically, malignant melanomas show multiple morphological patterns including epithelioid, spindle and round with various pigmentation from heavily pigmented to amelanotic [1].

Although previous studies have investigated various etiological factors including genetic mutations [2], exact mechanism of tumorigenesis remains unknown. While mucosal malignant melanomas are rare in human compared to those in dogs, their clinical outcome mimics canine mucosal malignant melanoma [1]. In addition, molecular genetic similarities are also present between canine and human mucosal melanomas including mutation of several driver genes [3]. Proto-oncogenes such as *MDM2* and *NRAS* or tumor suppressor genes like *TP53* are mutated at relatively same frequency. *BRAF* that is

mutated most commonly in human cutaneous melanoma is rarely mutated in both canine and human mucosal melanomas. On the other hand, another tumor suppressor gene *PTEN* is mutated at low frequency in canine mucosal melanoma despite relatively frequent mutation in human mucosal melanoma.

In human medicine, epigenetic mechanisms that refer to changes in phenotype without changes in genotype have been focused to be important factors in many diseases including neoplasia [4, 5]. One of the epigenetic modifications, DNA methylation is the conversion of cytosine to 5-methylcytosine at cytosine-guanine (CpG) dinucleotides, and DNA methylation at promoter region of genes represses gene transcription [6]. Although CpG sites are generally scattered throughout the genome, there are CpG dense regions known as CpG islands (CGIs). Whereas CpG sites in CGIs are typically unmethylated in normal tissues, it gets methylated in neoplasia. CGIs are located at promoter regions of about half of the genes in mammals [7] and de novo hypermethylation of tumor suppresser-genes in neoplastic tissues has been identified [8, 9]. On the other hand, majority of CpG sites in non-CpG islands are methylated in normal tissues, and DNA methylation is decreased in neoplasia [10].

In veterinary medicine, the number of studies for DNA methylation in canine neoplasia has been increasing [11]. Although there are several reports for DNA

methylation in canine malignant melanoma [12, 13], DNA methylation status in canine malignant melanoma is still unclear. Therefore, the aim of following studies is to reveal DNA methylation change in canine malignant melanoma from three different perspectives.

In chapter 1, I analysed genome-wide DNA methylation status that has not been reported in canine malignant melanoma using next-generation sequencing (NGS).

In chapter 2, I examined DNA methylation status of the Long Interspersed Nucleotide Element-1 (LINE-1) repetitive elements. LINE-1 is the most well recognized repetitive elements showing hypomethylation in various cancers [14] and could be used as a surrogate marker of genome-wide methylation changes [15].

Finally, I focused on the relationship between DNA methylation and epithelial mesenchymal transition (EMT). EMT is a reversible biologic process that epithelial cells gain mesenchymal properties including loss of intracellular adhesion [16]. In tumors, EMT plays a crucial role in tumor progression by inducing enhanced migratory capacity, invasiveness, and elevated resistance to apoptosis or therapeutic agents [17] and similar processes have been described in melanoma [18]. As EMT is a reversible process, epigenetic mechanisms that refer to a reversible modification are considered to influence EMT contributing to the reversible nature [19]. In chapter 3, I investigated the difference

in DNA methylation status between epithelial and mesenchymal phenotypes in canine malignant mucosal melanoma.

CHAPTER 1

Genome-wide DNA methylation analysis identifies promoter hypermethylation in canine malignant melanoma

Introduction

In human medicine, genome-wide analysis of DNA methylation revealed hundreds of genes with aberrant methylation in a variety of cancers, including malignant melanoma [4, 5]. Although there are several reports for DNA methylation in canine neoplasia [20, 21], including a few studies on canine malignant melanoma [13], most of these studies analysed one or two targeted genes that were reported in human medicine. Therefore, these studies could not clarify the extent to which genomic DNA methylation status is changed in these diseases.

In previous study, genome-wide DNA methylation analysis based on the next-generation sequencing (NGS) technique Digital Restriction Enzyme Analysis of Methylation (DREAM) in canine lymphoma cell lines showed that more than one hundred thousand CpG sites could be analysed using this technique [22]. The purpose of this chapter is to reveal widespread DNA methylation changes in canine malignant melanoma by using DREAM.

Materials and Methods

Samples

Six samples of normal oral mucosa from four healthy Beagles, four malignant melanoma cell lines (CMM1, CMM2, CMeC, and LMeC) [23, 24] and five clinical samples of malignant melanoma that were obtained at Veterinary Teaching Hospital in Rakuno Gakuen University and Gifu University were used in this study (Table. 1). The median age of dogs for clinical samples of melanoma was 13.5 years (range, 12.5–15 years), and they included three males and two females. Five melanoma clinical samples were labelled as MCS1, MCS2, MCS3, MCS4, and MCS5, respectively. Since a majority of canine malignant melanomas arise from oral mucosae, which were frequently used as controls in several previous reports [25, 26] in addition to the difficulty of obtaining adequate number of normal melanocytes, normal oral mucosae were selected as a control. The normal oral mucosae were labelled as OM-1 (buccal mucosa of dog 1), OM2-1 (gingiva of dog 2), OM2-2 (hard palate of dog 2), OM2-3 (buccal mucosa of dog 2), OM3 (gingiva of dog 3), and OM4 (buccal mucosa of dog 4). Collection and distribution of the samples were approved by the Institutional Animal Care and Use Committee (admission number; 15–0090, 15–0033) and conducted in accordance with the Hokkaido University

Animal Experimentation Regulations.

Digital restriction enzyme analysis of methylation

Genome-wide DNA methylation analysis using NGS was performed as previously [27] (Fig.1). Genomic DNA (2 μg) extracted from the samples was mixed with 2 pg of artificial methylation standards for calibrators (methylation levels of 0%, 25%, 50%, 75% and 100%). These mixes were sequentially digested with 100U *Sma*I endonucleases (New England Biolabs) for 3h at 25℃ and 50U *Xma*I endonucleases (New England Biolabs) for 16h at 37℃. The digested DNA was purified using Agencourt AMPure XP magnetic beads (Beckman Coulter). The 3′ recessed ends of the DNA created by digestion were filled in with a dCTP, dGTP and dATP mix (0.4 mM of each) and 3′-dA tails were added to all restriction fragments by Klenow DNA polymerase lacking 3′–5′exonuclease activity (New England Biolabs). Illumina paired-end sequencing adaptors were ligated using T4 DNA ligase (New England Biolabs). The ligation mix was size selected by Dual-SPRI size selection with Agencourt AMPure XP to obtain DNA fragments ranging from 250 to 450 base pairs (bp). Purified DNA was amplified with Illumina paired-end PCR primers using KAPA Hifi HotStart ReadyMix (Kapa Biosystems) and 11 cycles of amplification. The resulting sequencing library was cleaned with Agencourt AMPure XP

beads and sequenced on an Illumina HiSeq 2000 (Illumina). Sequencing reads were mapped to SmaI/XmaI sites in the canine genome (canFam3.1), and signatures corresponding to methylated and unmethylated CpGs were enumerated for each SmaI/XmaI site. Methylation frequencies for individual SmaI/XmaI sites were then calculated. The methylation ratio is the ratio of the number of tags starting with CCGGG divided by the total number of tags mapped to a given SmaI/XmaI site. Methylation levels measured by DREAM were corrected on the basis of the values obtained from the spikes in standards. Log ratios ln (m/u) and ln (sm/u) were calculated for each standard, where m/u is the expected ratio of methylated and unmethylated reads, while sm and u are observed numbers of methylated and unmethylated reads, respectively. Differences in the 'expected' minus 'observed' log ratios were calculated for each standard. Correction factor c was calculated as an antilog of the average log difference (expected – observed). Corrected methylation values were then computed as $100\% \times [c \times sm/(c \times [sm + u])]$ for each CpG site. At least 20 sequencing reads were used to analyze methylation levels at individual SmaI/XmaI sites. On the basis of technical replicate experiments, DREAM can distinguish differences in methylation of >10%, with a false discovery rate (FDR) of 2.4% [27]. For the definition of CpG islands, the University of California, Santa Cruz (UCSC) definition which are regions of DNA with GC content of 50% or greater, length >200 bp,

and ratio of the observed number of CG dinucleotides to the expected number (based on the number of Gs and Cs in the segment) greater than 0.6 [28] was applied. Sites at promoter regions are defined as being located within 1 kb from transcription start sites (TSSs) of given genes.

Tentatively, de novo hypermethylation of CpG sites in CGIs was defined as a more than 20% increase from the basal DNA methylation level (0–15%) [29, 30]. On the other hand, the tentative criteria for hypomethylation of CpG sites in non-CpG islands (NCGIs) was defined as a greater than 50% decrease from the basal DNA methylation level (80–100%) [31, 32].

Statistical analysis

Smooth-scatter plots were made, and Student t-test was performed using the statistical computing language R and PRISM (GraphPad Software, Inc., CA), respectively. Hierarchical clustering analyses were performed by ArrayTrack (https://www.fda.gov/science-research/bioinformatics-tools/arraytracktm-hca-pca-standalone-package-powerful-data-exploring-tools) with Ward's method.

Gene ontology analysis

Gene ontology analysis was performed using DAVID [33, 34]. DAVID analyses were performed online with a count of >10 and Benjamini–Hochberg-corrected p-values < 0.05.

Table 1. List of the samples (six normal oral mucosae, four malignant melanoma cell lines and five malignant melanoma clinical samples)

	Normal oral mucosa						Malignant melanoma cell lines		
	OM1	**OM2-1**	**OM2-2**	**OM2-3**	**OM3**	**OM4**	**CMM1**	**CMM2**	**CMeC**
Breed	Beagle	Beagle			Beagle	Beagle	Toy poodle	Mongrel	Chow
Age	2 years and 8 months	2 years and 8 months			7 years	7 years	12years	13years	11years
Sex	male	female			female	female	male		male

Malignant melanoma clinical samples					
LMeC	**MCS1**	**MCS2**	**MCS3**	**MCS4**	**MCS5**
Beagle	Shi Tzu	Miniature Dachshund	Pug	Miniature Dachshund	Toy poodle
9years	14years	15years	14years	12years and 6months	13years
female	male	male	male	female	female

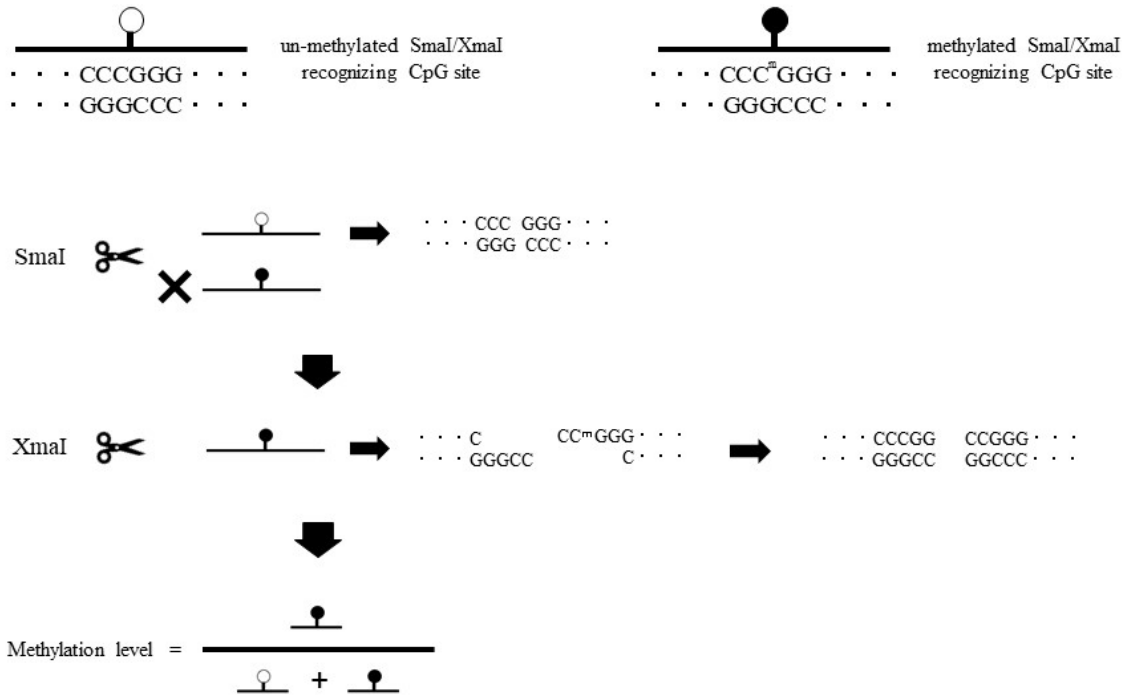

Fig.1. Schematic outline of the principle of DREAM

Both SmaI and XmaI enzymes recognize same site (CCCGGG). SmaI restriction endonucleases cut only unmethylated CCCGGG sites, creating GGG signatures. The remaining methylated CCC^{m}GGG sites are cut by XmaI restriction endonucleases with 3' recesses filled-in, resulting in CCGGG signatures. Sequencing adapters are ligated to SmaI/XmaI fragments and the libraries are subjected to next generation sequencing. Methylation levels at unique SmaI/XmaI sites are calculated based on the numbers of methylated and total signatures.

Results

Comparison of DNA methylation pattern among normal tissues or between normal tissue and malignant melanoma

A total of 9.1-30.4 million reads were generated from all 15 samples assayed for DNA methylation. Approximately 124,000–180,000 CpG sites with more than 20 reads were selected in each sample, and the 76,213 CpG sites in common across 15 samples were used for the downstream analyses (Table 2). All samples were compared to each other to observe the differences in DNA methylation patterns. First, high consistencies (Pearson $R^2 = 0.96$) were found among all pairs of normal tissues (Fig. 2a). On the other hand, pairs of normal oral tissue compared with melanoma cell lines and melanoma clinical samples showed low consistencies (Pearson $R^2 = 0.26$ and $R^2 = 0.57$), respectively (Fig. 2b, Fig. 2c).

DNA methylation changes in CGIs and NCGIs

CpG sites in CGIs and NCGIs were analysed separately to examine the differences in DNA methylation changes in each fraction. Of the 76,213 CpG sites, 29,482 were located in CGIs and 46,731 were located in NCGIs. The correlativity of all

15 samples was shown by hierarchical clustering analysis based on the genome-wide DNA methylation status and malignant melanoma were clearly separated from normal oral tissues in terms of both CGI and NCGI (Fig. 3). The DNA methylation patterns of the six normal oral tissues were clustered closer than that of malignant melanomas. In addition, melanoma cell lines and clinical samples were also separated clearly.

The four malignant melanoma cell lines and five malignant melanoma clinical cases were found to have 1054–4527 hypermethylated CpG sites in CGIs in comparison with normal tissues, which accounted for 4–15% of all CpG sites analyzed in CGIs or 9–37% of CpG sites with basal methylation levels in normal tissues, respectively (Table 3). On the other hand, 201-5597 hypomethylated CpG sites were found in NCGIs. These hypomethylated CpG sites constituted 1–25% of CpG sites with a basal methylation level in normal tissues among the NCGIs analyzed.

Gene ontology analysis

De novo hypermethylation in CGIs is a well-known phenomenon that correlates with gene expression silencing [35]. To gain insights into the characteristics of these hypermethylated CGI sites, their genomic coordinates were assessed to address the biological relevance of gaining DNA methylation in melanoma. Consequently, it was

found that 221–393 genes in melanoma cell lines and 81-120 genes in melanoma clinical samples had de novo hypermethylated sites at their promoter regions. Of these 221–393 genes in malignant melanoma cell lines, 179 genes were hypermethylated in all four melanoma cell lines (Table. 4). In addition, all five clinical samples had 26 hypermethylated genes, including 23 that were also hypermethylated in all malignant melanoma cell lines (Table. 5). Among these 23 genes, six genes annotated with "sequence-specific DNA binding" were significantly enriched (Table. 6).

Table 2. The number of unique usable reads and CpG sites covered by more than 20 reads of each sample for DNA methylation analysis with DREAM

Samples		Number of sequence reads	Number of CpG sites covered by more than 20 reads
Normal oral tissues	OM1	16,577,051	165,989
	OM2-1	18,378,225	151,069
	OM2-2	17,162,915	169,724
	OM2-3	24,946,812	180,110
	OM3	30,168,791	161,114
	OM4	30,380,530	174,169
Malignant melanoma cell lines	CMM1	22,501,331	142,776
	CMM2	20,423,191	152,555
	CMeC	14,839,086	179,278
	LMeC	17,021,958	124,195
Malignant melanoma clinical samples	MCS1	14,482,068	144,079
	MCS2	12,365,134	141,103
	MCS3	10,272,295	134,553
	MCS4	10,383,611	140,406
	MCS5	9,099,922	136,693

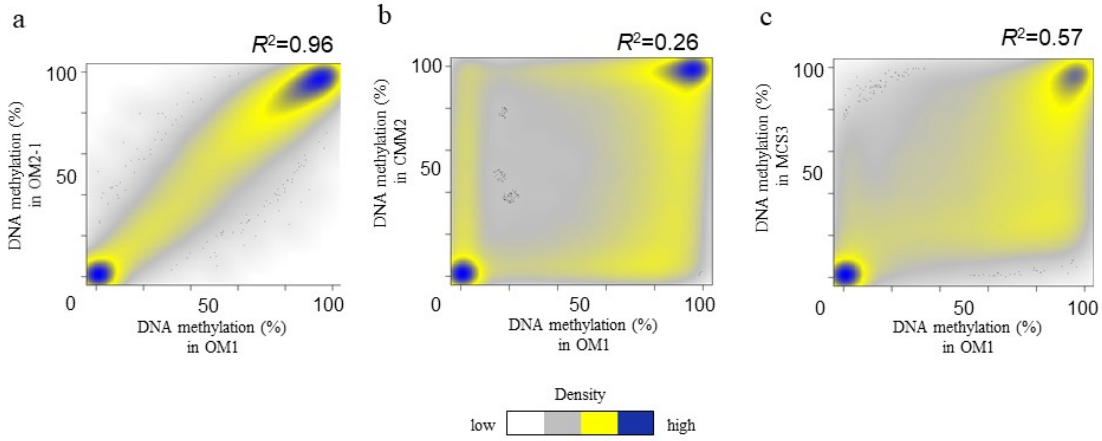

Fig. 2. Correlations and comparisons of DNA methylation status of normal oral mucosa from healthy dogs and canine malignant melanoma analysed by DREAM.

Representative smooth-scatter plots for DNA methylation levels of two normal oral mucosae (OM1 and OM2-1) (a), comparison between a malignant melanoma cell line (CMM2) and normal oral mucosa from a healthy dog (b), and a comparison between a malignant melanoma clinical sample (MCS3) and normal oral mucosa from a healthy dog (c). R^2 values are denoted in the upper right corner. DNA methylation level in normal oral mucosa from a healthy dog is plotted on the x-axis, DNA methylation levels in normal oral mucosa from a healthy dog, a malignant melanoma cell line, or a malignant melanoma clinical sample are plotted on the y-axis. The density of the number of CpG sites increases from white to grey to yellow to blue.

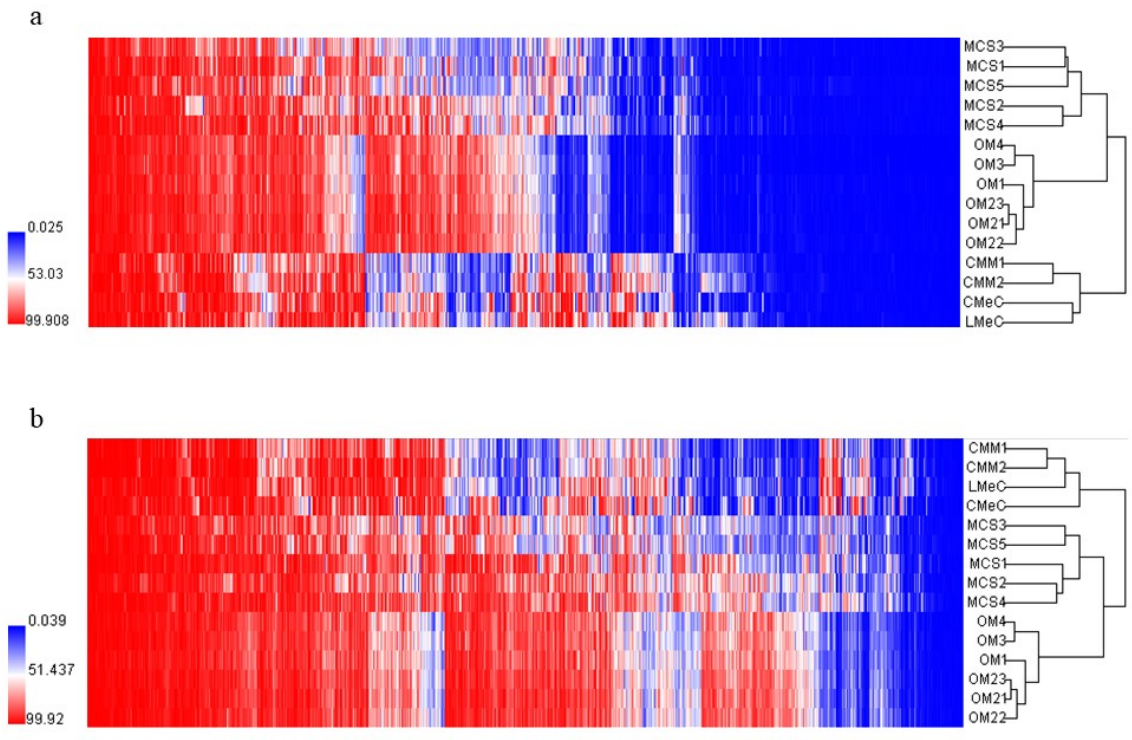

Fig. 3. Hierarchical clustering analysis of DNA methylation patterns of all 15 samples in CGIs (a) and NCGIs (b). Note that malignant melanomas are clearly separated from normal oral tissues. High and low DNA methylation levels are shown in red and blue, respectively, according to the colour scale, where 100 is fully methylated and 0 is unmethylated.

Table 3. The numbers and percentages of the hypermethylated CpG sites in CpG islands (CGI) in four malignant melanoma cell lines and five malignant melanoma clinical samples compared to normal oral mucosa from healthy dogs. Percentages of the hypermethylated CpG sites are shown in comparisons to all CpG sites analyzed in CGI (29,482 CpG sites) and CpG sites with basal methylation in normal tissues (12,286 CpG sites) respectively. The bottom row shows the number of genes which had de novo hypermethylated sites at their promoter regions.

	CMM1	CMM2	CMeC	LMeC
Number of hypermethylated sites	3650	4225	2922	4527
Percentage of hypermethylated sites	12%	14%	10%	15%
Percentage of de novo hypermethylated sites	30%	34%	24%	37%
Number of hypermethylated promoter genes	320	373	221	393

	MCS1	MCS2	MCS3	MCS4	MCS5
Number of hypermethylated sites	1378	1054	1197	1528	1226
Percentage of hypermethylated sites	5%	4%	4%	5%	4%
Percentage of de novo hypermethylated sites	11%	9%	10%	12%	10%
Number of hypermethylated promoter genes	103	81	89	120	92

Table 4. List of the genes with promoter hypermethylation in all four malignant melanoma cell lines

GDA	TMEM215	FGF19	cfa-mir-129-2	PNMT	TPH1
MYCL	IRX4	GALR1	cfa-mir-375	RHPN2	GRP
ASCL2	CA3	PCDH17	GAD1	FOXI2	AK7
PRKCH	NODAL	PRDM13	SOWAHB	DDN	PXDC1
MN1	NWD2	MAPK15	HOXC12	MYADML2	PNP
MATN4	LMX1A	OXTR	EMILIN2	BSX	ALPK3
EFNB3	LVRN	EVX1	EN2	ADAM23	LMAN1L
MCIDAS	CPNE9	CCL25	COL24A1	IKZF1	TRIM67
ECEL1	TRPA1	DMRT1	GCM2	MSC	PLBD1
SP5	VENTX	NIPAL4	IRX2	UCN	ICAM5
SCN3B	ADRB3	ADAMTSL3	PROKR2	TPM1	GPR6
SHANK2	PUS1	SYT6	PGR	DLX4	PRLHR
BCAT1	TMEM233	ALOX12	CCK	C1QL4	HOXC10
KIF26A	DUOX1	SAMD12	KDR	ADAM33	HNF1B
KCNV1	TLX2	KRT9	HHEX	MTLR	ACRBP
CH25H	GRIK3	TGFB2	OSR2	ZC2HC1C	MT2A
ATP2A3	SNCB	BMP3	TCF24	MMP23B	SPRYD7
MAL	GATA5	CCR10	SLC18A3	ATP13A3	NT5DC2
RASGRP2	CLDN3	SSTR1	NOL4	UPK3A	ARHGAP17
BEGAIN	C20orf85	NKX1-1	NR5A2	TRAF1	KCNJ12
VAT1L	TWIST2	ODF2	OTP	WFIKKN1	ARL5C
NR2E1	GDNF	JAKMIP3	GRHL2	ADCY2	CCNF
CRELD1	GABRB2	ADORA1	NPBWR1	TOX2	TSSK3
KCNK12	HHIP	APCDD1	AGAP1	COL9A3	EMILIN3
HELT	SLC17A8	CBLN4	GMPPA	MLPH	MSX1
EPO	HOXA11	PRDM14	C11orf87	HOXA9	APOE
SFRP2	NEUROD2	RNH1	SEMA3G	TCP11	PABPC1L
DSC2	HOXD11	FAM110C	GPR37	CHRNA3	TIRAP
NHLH2	ALDH1A3	HAP1	NEURL1	HMX2	PLEKHG4
KCNS2	NEUROG1	GRM7	POMC	HES5	

Table 5. List of the genes with promoter hypermethylation in all 5 malignant melanoma clinical samples or all 9 malignant melanoma samples (5 clinical samples and 4 cell lines)

Genes with promoter hypermethylation in all 5 malignant melanoma clinical samples	Genes with promoter hypermethylation in all 9 malignant melanoma samples (5 clinical samples and 4 cell lines)
UPK3A	UPK3A
NEUROG1	NEUROG1
TMEM215	NR2E1
NR2E1	OSR2
OSR2	GRHL2
GRHL2	HOXA9
HOXA9	TLX2
TLX2	SPRYD7
PALM	EMILIN3
SPRYD7	TMEM233
EMILIN3	PLBD1
TMEM233	HMX2
PLBD1	PRDM14
HMX2	CA3
PRDM14	ADAMTSL3
CA3	DUOX1
ESRP1	SOWAHB
ADAMTSL3	ATP13A3
DUOX1	ADCY2
SOWAHB	SSTR1
ATP13A3	HAP1
ADCY2	ARL5C
SSTR1	HNF1B
HAP1	
ARL5C	
HNF1B	

Table 6. List of the genes that was annotated with ‘sequence-specific DNA binding’ by gene ontology analysis (Benjamini-Hochberg-corrected p-values < 0.05)

HMX2	TLX2	GRHL2	HOXA9	NR2E1	OSR2

Discussion

In this study, genome-wide DNA methylation patterns of canine malignant melanomas by using NGS were investigated. First, by the comparison of six normal mucosa in DNA methylation patterns, subtle differences among samples were found, indicating no difference in methylation profile by anatomical sites in normal tissue. This finding is supported by a previous study wherein DNA methylation patterns were largely conserved throughout tissues [36].

Next, the differences in genome-wide DNA methylation patterns between normal tissues and malignant melanomas were assessed and malignant melanoma showed DNA methylation patterns clearly distinct from those of normal oral mucosa. These results were consistent with a previous report wherein the genome-wide DNA methylation profile of melanomas was clearly different from that of benign nevi [4]. Increased DNA methylation levels were observed in CGIs and reduced DNA methylation levels was noted in NCGIs in melanoma in this study, which corresponds to the findings in human cancer [37], suggesting. that the differences in DNA methylation patterns between normal oral mucosa and malignant melanoma are based on tumorigenic transformation.

DNA methylation in the CGI promoter region of genes is well known to repress gene transcription. Therefore, DNA methylation status of CpG sites in promoter CGIs was separately assessed. As a result, 2922–4527 and 1054–1528 de novo hypermethylated CpG sites that included 221–393 and 81–120 gene promoters were found in malignant melanoma cell lines and malignant melanoma clinical samples, respectively. These results are consistent with the findings of a previous report that showed hypermethylation in the upstream regions of a large number of genes in human cancers [38]. Of these hypermethylated genes, 23 were found to be hypermethylated in all melanoma cell lines and melanoma clinical samples, suggesting that these genes are prone to being hypermethylated in malignant melanoma. Of these 23 genes, genes annotated with "sequence-specific DNA binding" were significantly enriched, including the three Homeobox genes *HMX2*, *TLX2*, and *HOXA9*. Homeobox genes encode the homeodomain proteins, which regulate cell growth and differentiation [39]. In addition, Homeobox genes are polycomb targets that are frequently methylated [39-41] and dysregulated in tumours [42]. These findings suggest that the hypermethylated Homeobox genes found in this study may be involved in the tumorigenesis of canine malignant melanoma.

While multiple genes were hypermethylated in all malignant melanoma cell lines

and malignant melanoma clinical samples in common, the number of hypermethylated CpG sites and hypermethylated genes was higher in melanoma cell lines than in melanoma clinical samples. This phenomenon may be explained by the effects of culturing, because culturing has been shown to result in a large number of methylation changes [43]. The influence of culturing was also suggested by the higher methylation level of hypermethylated genes in melanoma cell lines compared to the melanoma clinical samples (Fig. 4). Another possible explanation is the contamination of normal cells in melanoma clinical samples, which might lower the DNA methylation level. However, this seemed to be less likely because the samples used in this study consisted almost exclusively of neoplastic cells confirmed by histopathology.

In this study, both hypermethylated CpG sites and hypermethylated genes were the most numerous in LMeC, which is derived from melanomas that metastasise to lymph nodes. Widespread CpG island promoter methylation, referred to as the CpG island methylator phenotype (CIMP), was first identified in human colorectal cancer followed by a variety of tumours in humans [43-46]. Interestingly, CIMP is also associated with advanced-stage human malignant melanoma [47]. Thus, CIMP-like patients could present as canine melanoma cases with a poor prognosis; however, more intensive studies with clinical canine melanoma samples are required for confirmation of this hypothesis. In

addition, 42 genes were exclusively methylated in LMeC, including *Kiss-1R*, which is a receptor of a suppressor of metastasis, *Kiss-1*. The *Kiss-1* gene was initially discovered in malignant melanoma [48] and its suppressor function had been also described in various other cancers, including breast cancer, oesophageal carcinoma, and pancreatic and prostate cancers, with the suggested mechanism that MMP–9 is reduced through the downstream pathway of the Kiss-1/Kiss-1R complex [49].

Although malignant melanoma showed a large number of hypermethylated regions relative to that in normal oral mucosa, the effects of aberrant DNA methylation on gene expression changes and their relevance to tumorigenesis were not assessed in this study. In fact, hypermethylation of Homeobox genes was also observed in lymphoma cell lines in the previous study [22], implying that a part of hypermethylation in this study may be shared in canine tumours. In addition, most genes are inactive in gene expression in normal tissue before de novo methylation occurred in cancer cells [50], suggesting that DNA methylation of genes is not necessarily a cause but solely a consequence of oncogenesis. To address this issue more directly, the functional relevance of these methylated sites to melanoma tumorigenesis needs to be investigated by silencing the expression of the relevant genes in future studies.

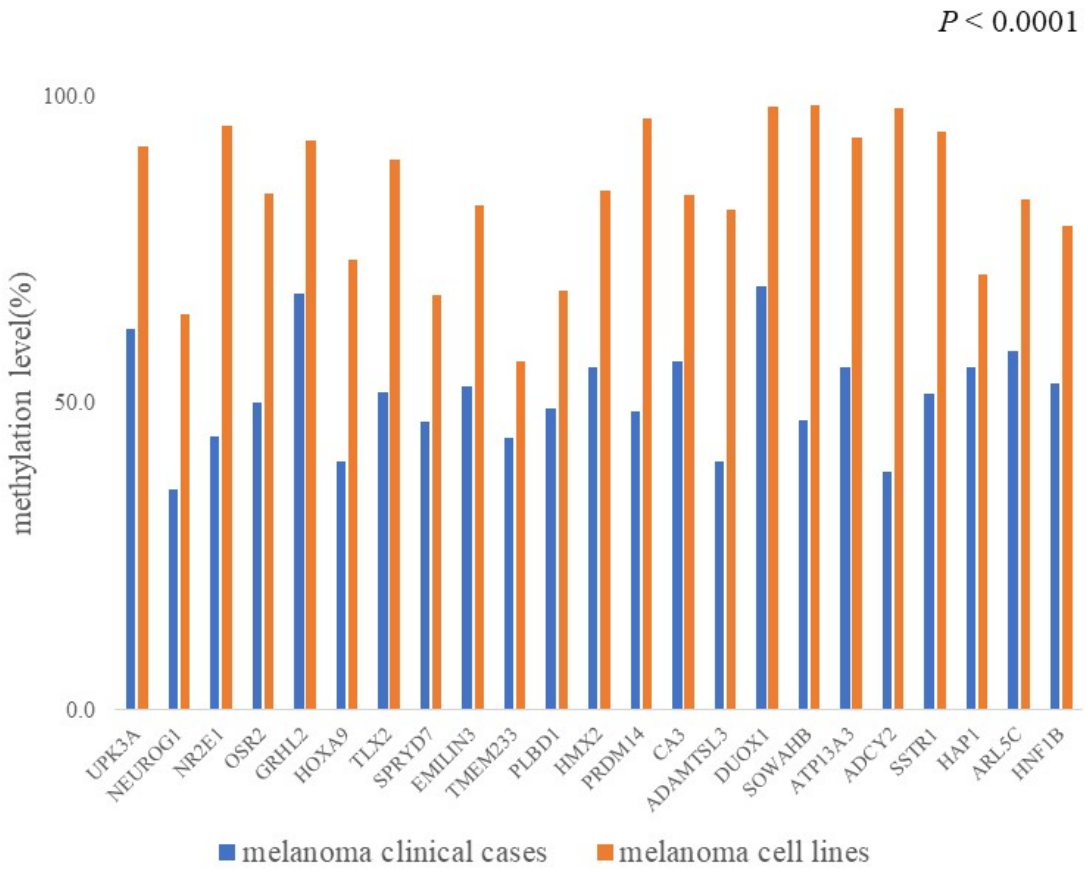

Fig. 4. DNA methylation levels of 23 genes that were hypermethylated in all melanoma cell lines and melanoma clinical samples. DNA methylation level of each gene was the average of cell lines (n = 4) and clinical samples (n = 5). Note that melanoma cell lines showed higher methylation levels than melanoma clinical samples in all genes. *P*-value was obtained by Student's t-test.

Summary

In this chapter, genome-wide DNA methylation analysis in malignant melanoma cell lines and clinical samples was performed by using DREAM. Increased DNA methylation levels were observed in CGIs and reduced DNA methylation levels were noted in NCGIs. In addition, a large number of hypermethylated genes were identified, suggesting the presence of widespread DNA methylation alterations in canine malignant melanoma. Although the functional effects of the observed DNA methylation changes need to be assessed, these signatures of aberrant DNA methylation could be used as early diagnostic or prognostic markers in canine malignant melanoma, similar to their utilisation in several cancers in human medicine.

CHAPTER 2

Long interspersed nucleotide element-1 hypomethylation in canine malignant mucosal melanoma

Introduction

In chapter 1, widespread DNA methylation alterations was detected in canine malignant melanoma by genome-wide DNA methylation analysis. Those DNA methylation changes include reduced DNA methylation levels in NCGIs in addition to increased DNA methylation levels in CGIs. Global hypomethylation occurs frequently in tumors and may facilitate chromosome instability, leading to the formation of abnormal chromosomal structures [51]. In this regard, the Long Interspersed Nucleotide Element-1 (LINE-1) repetitive elements are the most well recognized repetitive elements that account for about 17 % of human genome, showing hypomethylation in various cancers [14] and could be used as a surrogate marker of genome-wide methylation changes [15]. Interestingly, LINE-1 hypomethylation was also associated with prognosis in several human cancers [52-54]. Furthermore, given the abundance of LINE-1 elements in the genome, minimum amounts of DNA are required for their amplification and analysis. In fact, DNA methylation status of LINE-1 has been suggested to be a biomarker for several cancers even in the samples derived from plasma [55] as well as blood [56].

LINE-1 DNA methylation has previously been shown to be a diagnostic marker in dogs with mammary tumors [57]. However, to the best of our knowledge, no study has

investigated LINE-1 DNA methylation in canine malignant melanoma. Accordingly, the purpose of this study was to reveal DNA methylation status of LINE-1 in dogs with malignant melanoma and possible relationship of their DNA methylation level and survival of the patients.

Material and methods

Samples

Four malignant melanoma cell lines (CMM1, CMM2, CMeC, LMeC) [23, 24] and 41 clinical samples from dogs that presented to Veterinary Teaching Hospitals in Hokkaido University, Rakuno Gakuen University, Gifu University, and Azabu University between September 2013 and November 2019 were included in this study (Table 1). The median age of these dogs was 11.8 years (range, 8-16 years), and they included 27 males and 13 females (one with missing data). Histopathologic diagnosis was carried out by an American College of Veterinary Pathologists board-certified pathologist in most of the samples studied. Written informed consent was obtained from all owners of dogs involved in this study. Of 41 dogs, 12 dogs had insufficient data for follow-up or other causes of death, leaving 29 dogs for survival analysis. The survival rates were obtained from owners or medical records.

As in chapter 1, normal oral mucosae were used as a control (in this chapter, four normal oral mucosae from two healthy dogs were utilized). The animal use was approved by the Institutional Animal Care and Use Committee, Hokkaido University (Approval number: 15–0090).

Quantitative DNA methylation analysis

Bisulfite pyrosequencing was used to quantitatively assess DNA methylation [58] for promoter CGI of canine LINE-1. Briefly, genomic DNA (500 ng) extracted from the samples was used for bisulphite conversion by using the innuCONVERT Bisulfite Basic Kit (Analytika yena) according to manufacturer's instructions. To select the primers to amplify canine LINE-1 fragments, canine LINE-1 was retrieved from Repbase [59] and a putative promoter on CGI was identified (Fig, 1). Then, primers that are capable of amplifying as many canine LINE-1 fragments as possible were searched in in silico analysis by UCSC In-Silico PCR. Primer sequences used for the amplification and sequence of the promoter region of LINE-1 are as follows; Forward, TAGAGGTAGGGAGGGTTTAGGATA; Reverse-biotin, (biotin)-CCCCAATAACCAAACAACTCTA; Sequence, TTGTTTTAGTTGAGTAGATT. The following PCR conditions were used: initial denaturation at 94°C for 3 minutes, followed by 40 cycles comprising denaturation at 94°C for 30 seconds, annealing at 50°C for 30 seconds, and extension at 72°C for 30 seconds. Forty cycles were used to completely exhaust the biotinylated primer.

Levels of DNA methylation were measured as the percentage of bisulphite-resistant cytosines at CpG sites by pyrosequencing using a PSQ24 system with Pyro-Gold

reagent Kit (QIAGEN), and the results were analyzed using PyroMark Q24 software (QIAGEN). The pyrosequencing assay interrogates two adjacent CpG sites and DNA methylation levels were calculated by the average of these two sites.

Statistical analysis

DNA methylation levels among the different groups were compared using One-way ANOVA with unpaired, nonparametric, Kruskal-Wallis test with Dunn's multiple comparisons test. P value <0.05 was considered statistically significant. The association between LINE-1 methylation level and overall survival (OS) in melanoma patients was assessed using the Kaplan–Meier method and the log-rank test. P value < 0.05 was considered statistically significant. I also used Cox proportional hazards model for multivariate regression analysis with covariates such as age, gender, and WHO stage along with LINE-1 DNA methylation level as a continuous variable. Statistical analysis was performed using PRISM 6 (GraphPad Software, Inc., California) and MedCalc for Windows, version 13.0 (MedCalc Software, Ostend, Belgium).

Table 1. Characteristics of patients

	Breed	Age	Gender	Site	Primary tumor	Regional lymph nodes	Distant metastasis	Staging	Treatment	Dose of radiation therapy	Survival (days)	Censored (reason)
1	Chihuahua	15	M	oral	T2	N0	M0	II	Intracapsular	NA	194	Lost contact
2	American Coker Spaniel	13	M	oral	T2	N1	M0	III	Radical	NA	55	Renal failure
3	Labrador retriever	16	F	oral	T3	N0	M0	III	NA	NA	NA	NA
4	Miniature Dachshund	12	M	oral	T3	N1	M1	IV	C, R	3*8 Gy/week	108	
5	Chihuahua	11	F	oral	T1	N0	M0	I	Wide	NA	429	Lost contact
6	Hokkaido	14	F	tongue	T1	N1	M1	IV	Intracapsular, C, R	4*6 Gy/week	302	
7	Shiba	NA	M	palate	NA	N0	M0	NA	NA	NA	NA	NA
8	Miniature Dachshund	14	M	submandibular lymph node	T3	N0	M0	III	NA	NA	NA	NA
9	Pug	14	M	oral	T2	N0	M0	II	Marginal, R	1*8 Gy/week	91	
10	Mix	12	M	tongue	T2	N0	M0	II	Marginal, C	NA	330	
11	Toy poodle	13	F	oral	T2	N1	M0	III	Wide	NA	183	In follow-up
12	French bulldog	11	M	palate	T2	N0	M0	II	Marginal, C, R	4*6 Gy/week	131	Lost contact
13	Border Collie	10	M	oral	T1	N0	M0	I	Wide, R	5*7 Gy/week	195	Concurrent lymphoma

14	Shepherd	9	F	oral/tongue	NA	N0	M0	NA	Marginal	NA	NA	NA
15	Mix	12	M	lip	NA	N0	M0	NA	Marginal	NA	214	
16	Mix	15	M	oral	T3	N0	M0	III	R	3*8 Gy/week	23	
17	Miniature Schnauzer	12	F	oral	T3	N1	M0	III	Marginal	NA	NA	NA
18	Labrador retriever	11	M	oral	T3	N0	M0	III	NA	NA	549	
19	Shepherd	11	M	oral	T3	N1	M0	III	Marginal, R	4*8 Gy/week	57	Lost contact
20	Pomeranian	13	M	oral	T2	N0	M0	II	NA	NA	459	
21	Golden retriever	10	M	oral	T1	N1	M0	I	Wide	NA	46	
22	Shi Tzu	14	M	oral	T3	N0	M0	III	R	3*8 Gy/week	24	Lost contact
23	Pug	12	F	oral	T2	N0	M0	II	Marginal	NA	615	
24	Flat coated retriever	9	M	oral	T3	N1	M0	III	Intracapsular, R	NA	127	
25	Miniature Dachshund	12	F	oral	NA	N1	M0	NA	NA	NA	NA	NA
26	Mix	9	F	lip	NA	N1	M1	IV	Marginal, R	5*7 Gy/week, 6*6.3 Gy/week	324	Concurrent HCC
27	Labrador retriever	13	F	palate	T2	N0	M0	II	Marginal	NA	NA	NA
28	Miniature Dachshund	10	M	oral	NA	N0	M0	NA	NA	NA	NA	NA
29	Miniature Dachshund	12	F	oral	T2	NA	NA	NA	R	2*8 Gy/week, 4*6.3 Gy/week	770	

30	Miniature Dachshund	9	M	oral	NA	N0	M0	NA	NA	NA	NA	NA
31	Miniature Dachshund	15	M	lip	T2	N1	M0	III	Marginal, R	NA	26	
32	Mix	12	M	palate	T3	N1	M1	IV	Intracapsular, R	5*8 Gy/week	218	
33	Shetland sheepdog	8	M	oral	T2	N0	M0	II	Marginal, C	NA	1079	
34	Shetland sheepdog	10	M	tonsil	T3	N0	M0	III	Marginal, R	4*8 Gy/week	226	
35	Flat coated retriever	9	F	oral	T2	N0	M0	II	Marginal, R	6*8 Gy/week	183	Concurrent HS
36	Labrador retriever	12	F	tongue	T3	N0	M0	III	NA	NA	NA	NA
37	Labrador retriever	11	NA	oral	NA	N0	M0	NA	NA	NA	1000	In follow-up
38	Shetland sheepdog	10	M	lip	T2	N0	M0	II	Marginal, R	5*6.3 Gy/week	348	In follow-up
39	Mix	10	M	tongue	T3	N0	M0	III	S, R	4*6.3 Gy/week	636	
40	Miniature Dachshund	12	M	oral	T3	N0	M0	III	Intracapsular, R	4*6 Gy/week	166	
41	Papillon	13	M	oral	T2	N0	M0	II	Intracapsular, R	NA	170	

Abbreviations: C, chemotherapy; D, detected; F, female; HCC, hepatocellular carcinoma; HS, histiocytic sarcoma; M, male; NA, not available; ND, not detected; R, radiatio

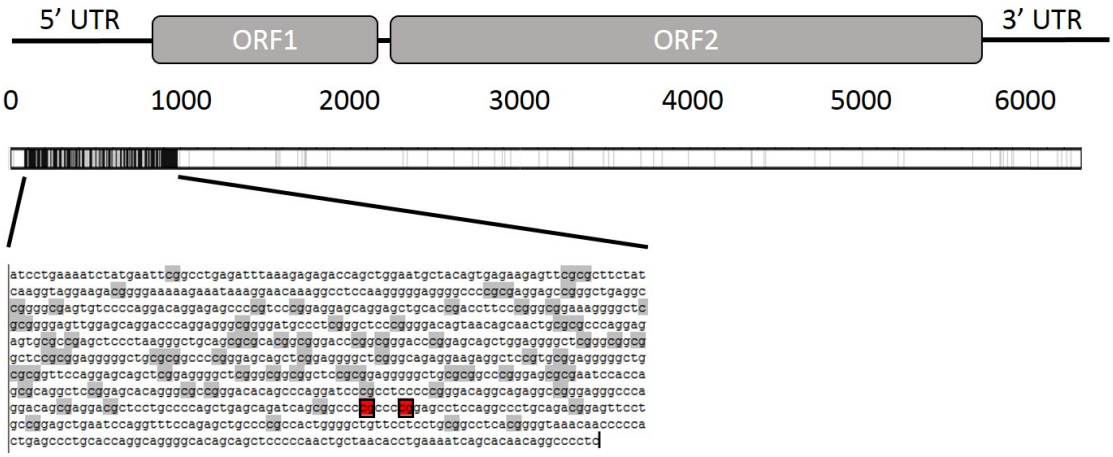

Fig. 1. Structure of canine LINE-1 and the location of CpG sites analyzed in this study. (Upper) Canine LINE-1 (6298 bp) structure including 5’UTR and 3’UTR is shown. ORF; Open reading frame. (Middle) CpG sites and CpG island are shown by vertical gray lines and a black rectangle, respectively. (Lower) Sequence of the CpG island at the putative promoter region of canine LINE-1. CpG sites in the region are shown in gray. The two CpG with rectangles are analyzed by bisulfite-pyrosequencing in this study.

Results

DNA methylation status of LINE-1 in canine melanoma patients, cell lines, and normal mucosae

DNA methylation status of LINE-1 was successfully measured in all samples by bisulfite-pyrosequencing. The detailed clinical data of 41 clinical melanoma patients are available in Table 1.

Representative pyrograms where two adjacent CpG sites located at the promoter regions of canine LINE-1 were shown in Fig.2. First and second CpG site showed 75% and 78% of DNA methylation level, respectively, in the normal mucosa. On the other hands, one of the cell lines showed lower methylated status 57% and 60% in the same regions. These two CpG sites showed parallel DNA methylation levels in most of the samples studied.

Next, all samples including six melanoma cell lines and 41 melanoma patients were analyzed (Fig.3). Interestingly, methylation status of normal mucosae was found to be ranging from 74% to 76%, whereas melanoma cell lines showed 58% to 64%. In addition, DNA methylation status of the majority of spontaneous melanoma samples ranged from 23% to 82% and statistically lower methylation levels compared with normal

mucosae (p=0.012).

Relationship between LINE-1 methylation and survival duration

The relationship between LINE-1 methylation and survival duration was analyzed using 31 melanoma patients where clinical information were available. A threshold was temporarily defined to be 65%, which is 10% lower methylation levels than those in normal mucosae (75%). As a result, LINE-1-low patients (N=19) showed worse overall survival compared with LINE-1-high patients (N=12), though the difference did not reach statistical significance (p=0.09, Fig. 4A). No difference was found regarding gender and the frequency of having metastasis at the time of diagnosis (p=1.00, Fig.4B and 4C). LINE-1-high patients were found to be younger than LINE-1-low patients (p=0.04, Fig. 4D). However, multivariate regression analysis did not reveal that LINE-1 DNA methylation level was independently associated with OS (p=0.24).

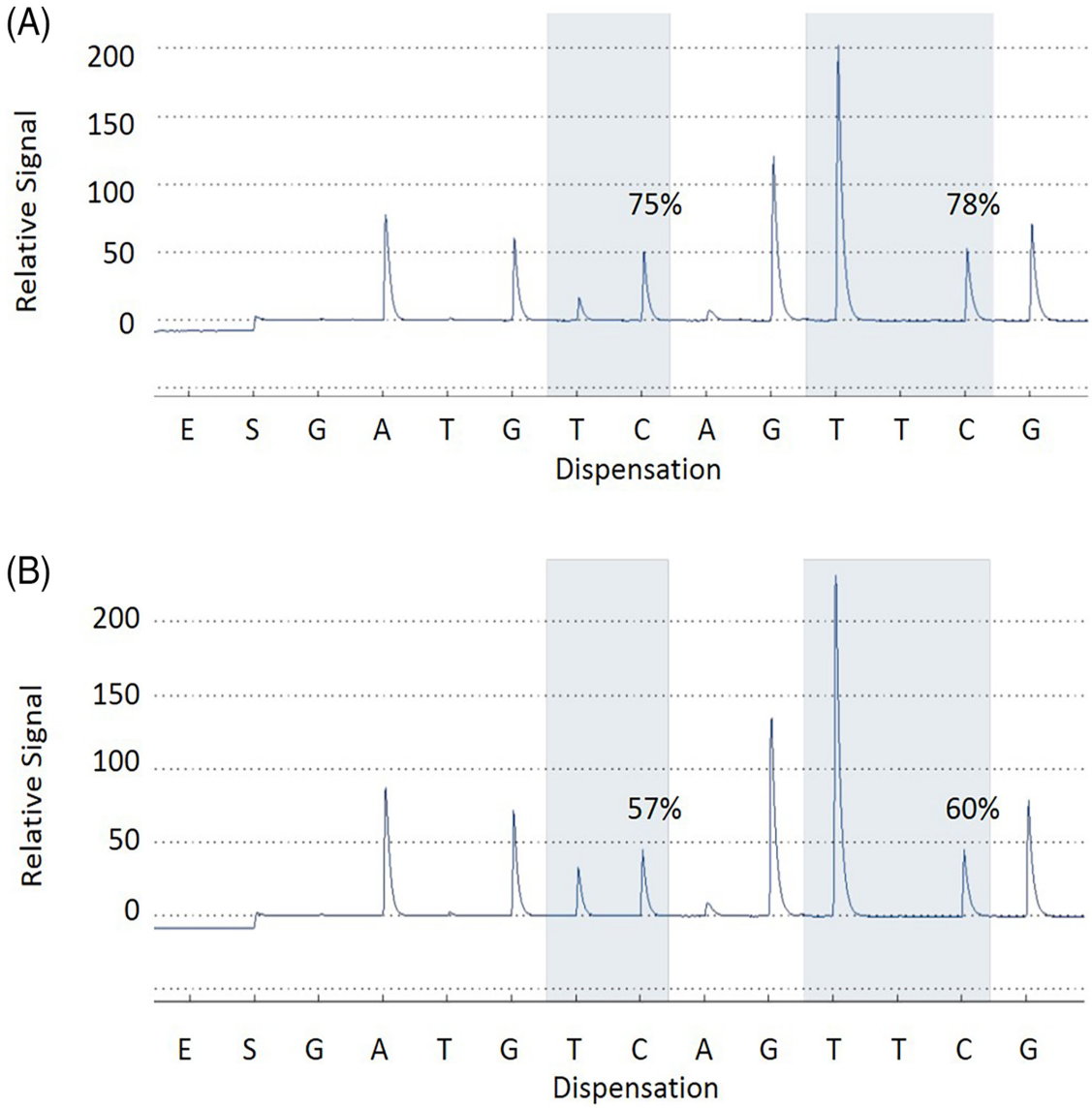

Fig. 2. Pyrograms. Examples of pyrograms are shown for low methylation densities in the normal mucosa sample (A) and melanoma cell line (CMM2) (B) for LINE-1. Two CpG sites are highlighted in gray. Enzyme (E) and substrate (S) are added before nucleotides for the sequence to analyze according to the dispensation order.

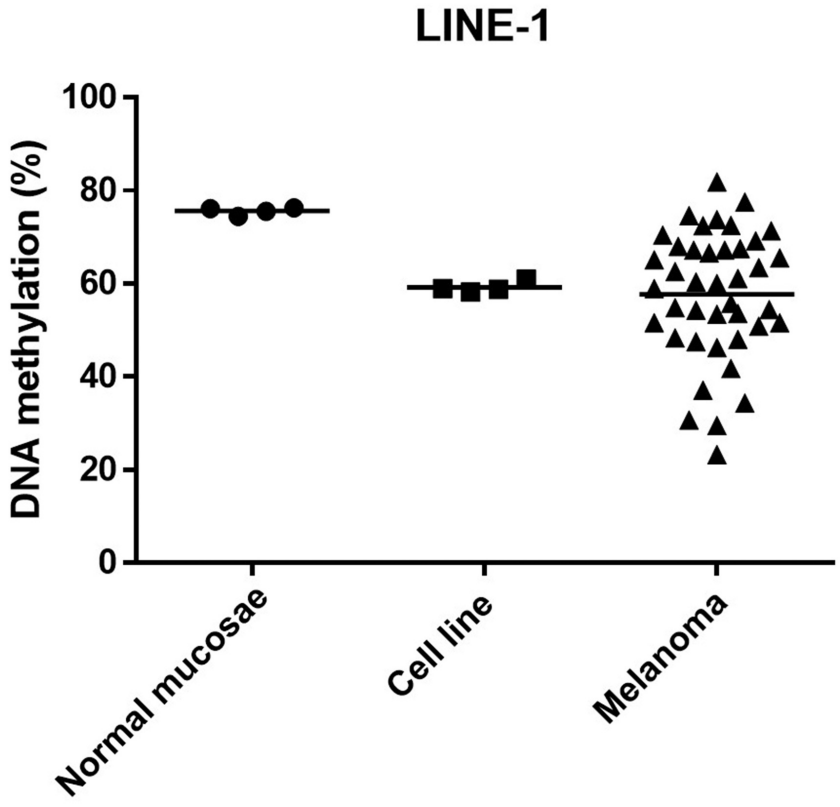

Fig. 3. DNA methylation levels of canine LINE-1 in samples from normal mucosae, melanoma cell lines, and spontaneous melanoma patients. Melanoma cell lines and spontaneous melanoma patients showed lower methylation level compared to normal mucosae.

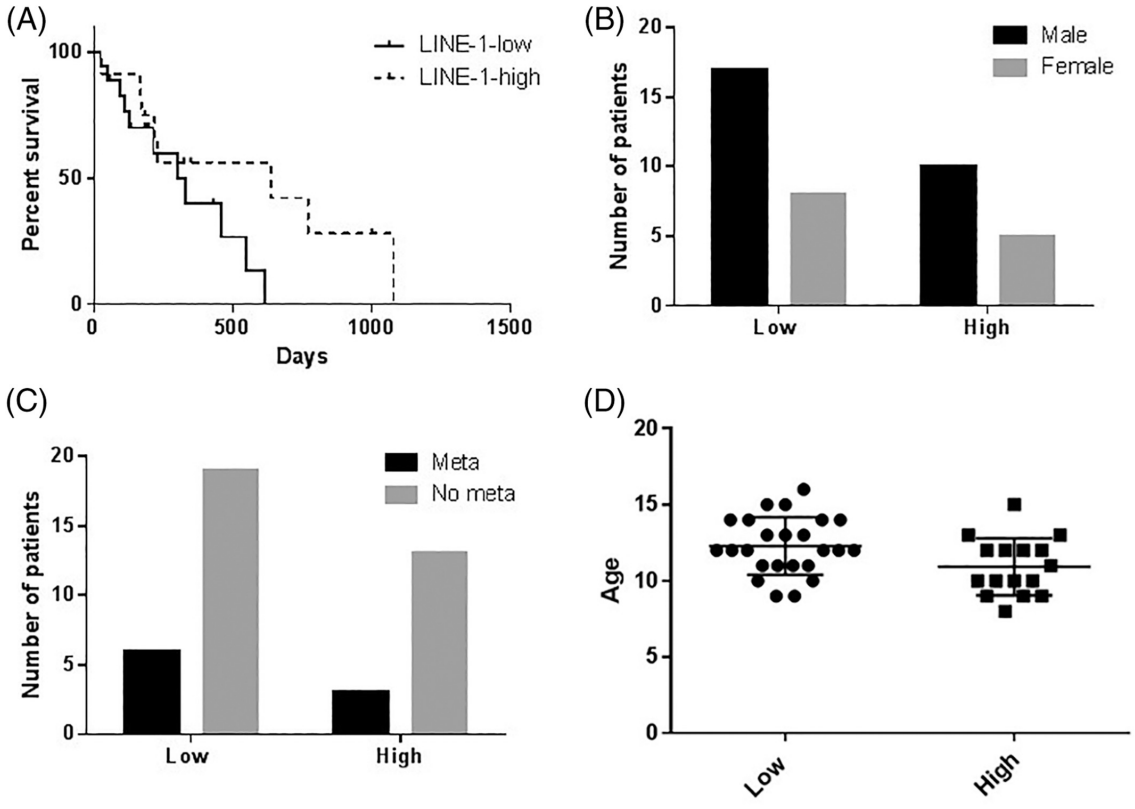

Fig. 4. Characteristics of LINE-1-low and LINE-1-high patients. (A) Kaplan-Meier survival curves for LINE-1-low and –high patients are indicated by the solid line and the dotted line, respectively. LINE-1-low patients (N=19) showed trend of having worse overall all survival compared with LINE-1-high patients (N=12) (p=0.09). p values are derived from the log-rank test. Status of gender (B), metastasis status (C), and age (D) are shown for LINE-1-low and LINE-1-high patients.

Discussion

In this chapter, DNA methylation status of LINE-1 in canine malignant melanoma samples was investigated using bisulfite-pyrosequencing which is a highly sensitive and high-throughput method to quantify CpG site methylation for a large number of samples [58].

First, four samples of normal oral mucosae were found to be highly methylated. This is consistent with the fact that human normal tissues have shown methylated status at LINE-1 [14] and canine normal mammary tissues had previously been found methylated for LINE-1 by methylation-sensitive restriction enzyme digestion followed by real-time PCR [57]. Next, it was found that LINE-1 in canine melanoma patients ($p=0.001$) and melanoma cell lines ($p=0.01$) are hypomethylated compared to normal mucosae. These results were also consistent with a previous report in humans where DNA methylation profile of LINE-1 promoter in melanoma was clearly different from that of skin [54].

There are several lines of possible association between the hypomethylation of LINE-1 and canine melanoma samples. First, global DNA hypomethylation could be indicated by LINE-1 hypomethylation and is suggested to be associated with cancer

development through genomic and chromosomal instability in tumors [60]. Alternatively, overexpression of oncogenes that could lead to the cause of tumorigenesis was also postulated to be a result of this hypomethylation [35]. In chapter 1, it was found that canine melanoma cell lines and clinical samples showed drastic de novo DNA hypermethylation in CGI promoter region that covered thousands CpG sites and hundreds of genes. Despite this hypermethylation of multiple genes in canine melanoma, unequivocal hypomethylation was also noted for thousands of CpG sites in non-CGI regions. Therefore, hypomethylation of LINE-1 repetitive elements in this chapter could be a representative global hypomethylation occurred in canine malignant melanoma. Although it remains to be demonstrated whether genome-wide hypomethylation and LINE-1 hypomethylation would be correlated in the samples from canine clinical malignant melanoma patients, quantitative analysis of LINE-1 DNA methylation level by bisulfite-pyrosequencing could offer a surrogate marker for the extent of global hypomethylation in a time- and cost-effective manner.

In this study, it was also demonstrated that global levels of LINE-1 methylation of canine malignant melanoma seemed to be a predictor of OS. This finding suggests remarkable clinical relevance by providing the first evidence of a molecular epigenetic marker with prognostic value in canine malignant melanoma patients. Human stage III

melanoma patients can be divided into two groups according to LINE-1 methylation; however, patients with lower methylation of LINE-1 were found to have significantly better prognosis than those with higher methylation [54]. Interestingly, LINE-1 hypomethylation was also associated with a poorer prognosis in human colon and ovarian cancer [52, 53]. Thus, it is suggested that the underlying effect of LINE-1 hypomethylation on clinical outcome is tumor-type dependent.

Canine malignant melanoma has a variety of prognostic factors including signalment, clinical features of the patients, and tumor characteristics [61]. In this study, no enrichment of the patients with LINE-1-low were noted regarding gender and metastasis found at the time of diagnosis. This suggests that the global hypomethylation event is independent of these features. Instead, LINE-1-high patients were found to be younger than LINE-1-low patients though patients' age has not reported to have definitive prognostic significance [61]. Relationship of LINE-1 DNA methylation status with other important biological and histological features such as Ki67 index and degree of pigmentation needs to be investigated in future study, since these are unavailable in the samples used in this study.

The underlying biological mechanism through which hypomethylation of LINE-1 in canine malignant melanoma is associated with a poorer survival was not investigated

in this study. Estecio *et al.* demonstrated in the study of human colon cancer that patients without microsatellite instability (MSI) had a significant decrease in LINE-1 DNA methylation compared to MSI-positive patients [14]. MSI-positive as well as LINE-1 DNA methylation are positively associated with an increase in number of tumor-infiltrating lymphocytes (TILs) in esophageal and colorectal cancer [62, 63], suggesting that TILs induced by high level of LINE-1 methylation and/or MSI-positivity through an unknown mechanism could play a role in the potential interaction between inflammatory mediators and tumors for determination of the fate in patients' prognosis.

Although DNA methylation status of LINE-1 was conducted in the samples from malignant melanoma tissues and normal oral mucosa, the effects of different cell-context in the samples on DNA methylation level cannot be ruled out. Normal cells in tumor samples might affect LINE-1 DNA methylation level so that hypomethylation would possibly be underestimated unless tumor samples are completely normal cell-free. Therefore, one might need to exercise caution not to select LINE-1-high patients to predict better prognosis. Instead, patients showing LINE-1 hypomethylation should be considered to have a worse prognosis in this context.

Summary

In this chapter, quantitative analysis of LINE-1 DNA methylation level was conducted by bisulfite-pyrosequencing in canine oral malignant melanoma samples. Malignant melanoma showed hypomethylation of LINE-1 compared to normal tissue corresponding to the reduced DNA methylation levels in NCGIs that was noted in chapter 1. In addition, lower methylation level of LINE-1 is associated with poorer survival in canine malignant melanoma. These results indicated that LINE-1 DNA methylation level could be used as a surrogate marker of global methylation level and prognosis in canine oral malignant melanoma.

CHAPTER 3

Differences in DNA methylation status between epithelial and mesenchymal phenotypes in canine malignant mucosal melanoma

Introduction

As mentioned in the general introduction, canine oral malignant melanoma is a highly aggressive and metastatic tumor with a high degree of pathological heterogeneity, presenting various morphological patterns such as epithelioid and spindle cells. Epithelioid and spindle cells often coexist in a single neoplastic tissue [3]. This finding indicates that neoplastic cells change their morphology during tumor progression. Epithelial–mesenchymal transition (EMT) has been considered an important mechanism underlying morphological changes. EMT is a reversible biological process in which epithelial cells gain mesenchymal properties, including the loss of intracellular adhesion [16]. EMT is a central event required for mesoderm and neural tube formation during embryogenesis [16].

Under pathological conditions, particularly in tumors, EMT plays a crucial role in tumor progression by inducing enhanced migratory capacity, invasiveness, and elevated resistance to apoptosis or therapeutic agents [17]. EMT is regulated by a network of several signaling pathways, such as Notch and Wnt signaling, which are induced by hypoxia [64]. Although EMT is the most well-known process in epithelial cell tumors, similar processes have been described in non-epithelial cancers, including melanoma,

with increased metastatic propensity and decreased sensitivity to therapy [18]. EMT has been reported in canine malignant melanoma, which is characterized by decreased expression of the cell adhesion molecule E-cadherin [65] and increased expression of transcription factors such as ZEB and Snail [66]. In addition, E-cadherin expression in canine oral melanoma is associated with pigmentation and clinical outcome [65].

As EMT is a reversible process, epigenetic mechanisms that refer to reversible modifications are considered to influence EMT, contributing to its reversible nature [19]. Although several studies on human cancer have indicated a correlation between EMT and DNA methylation [67], there are no reports regarding the effect of DNA methylation on EMT in canine tumors.

In this chapter, differences in DNA methylation status between epithelial and mesenchymal phenotypes in canine oral malignant melanoma were investigated.

Materials and Methods

Samples

This study was performed using six samples of normal oral mucosa from four healthy beagles that were included in the study presented in Chapter 1 and 28 clinical samples from dogs that were presented at Veterinary Teaching Hospitals in Hokkaido University, Rakuno Gakuen University, Gifu University, and Azabu University between September 2013 and November 2019 (Table 1). The median age of these dogs was 11.4 years (range, 8-15 years), and they included 17 male dogs and 10 female dogs (one with missing data). Histopathologic diagnosis was performed by an American College of Veterinary Pathologists board-certified pathologist for most of the samples studied. Written informed consent was obtained from all owners of dogs involved in this study.

The collection and distribution of samples were approved by the Institutional Animal Care and Use Committee (admission number: 15–0090, 15–0033) and conducted in accordance with the Hokkaido University Animal Experimentation Regulations.

Digital restriction enzyme analysis of methylation

Genome-wide DNA methylation analysis using DREAM was performed for the

above samples according to the procedure described in Chapter 1.

Immunohistochemistry

Ten samples were deparaffinized, rehydrated, and washed with distilled water. Antigen retrieval for E-cadherin was performed using microwave treatment with preheated Tris-EDTA buffer solution (10 mM–1 mM, pH 9.0) for 15–20 min at the lowest power. Endogenous peroxidase activity was blocked with 3% H_2O_2 in distilled water for 5 min at room temperature and the slides were washed 2–3 times in phosphate-buffered saline (PBS). The sections were incubated for 30 min at room temperature with the primary antibody, mouse monoclonal anti-E-cadherin (E-cadherin/CDH1 antibody, 4A2C7; Invitrogen, Carlsbad, CA, USA) at a dilution of 1:100. The slides were washed 2–3 times in PBS and incubated with a secondary antibody (MAX-PO (MULTI), Nichirei Bioscience Inc., Tokyo, Japan) for 30 min. After the slides were washed 2–3 times in PBS, they were incubated with peroxidase-labeled streptavidin for 5 min and washed in distilled water. 3,3'-Diaminobenzidine (DAB) and hematoxylin were used as the chromogen and counterstain, respectively. After being washed in distilled water, the coverslips were mounted in an aqueous medium. Normal canine mammary tissue containing ductal epithelial cells (epithelial component) and connective tissue

(mesenchymal component) was used as the control. Two board-certified pathologists from the Japanese College of Veterinary Pathologists blindly and independently assessed E-cadherin immunolabeling. The slides were evaluated for the percentage of E-cadherin-positive neoplastic cells and the intensity of immunolabeling (low [absent/mild], intense [moderate/marked]).

Western blotting

24 samples were mechanically homogenized and total protein was extracted using SDS lysis buffer (2% SDS, 50 mM Tris-HCl (pH6.8), 1 mM EDTA (pH 8.0)). The supernatant of the minced tumor tissues was then sonicated using BRANSON Sonifier 450 (Branson Ultrasonics Corporation, CT, USA) for 2 seconds at power 2. Protein concentrations were measured with TaKaRa BCA Protein Assay Kit (#T9300A, Takara Bio, Kusatsu, Japan) before adding 4× sample loading buffer (200 mM Tris-HCl buffer (pH 6.8), 8% SDS, 40% glycerol, 1% bromophenol blue, 20% 2-mercaptoethanol) and denaturing at 98°C for 5 min. Proteins were separated by electrophoresis (SDS-PAGE) in a polyacrylamide gel in presence of sodium dodecylsulfate (SDS) and transferred to Immobilon-P transfer membranes (#IPVH00010, Merck Millipore, MA, USA). Membranes were blocked with 5% skimmed milk in Tris-buffered saline with 0.05%

Tween 20 (TBST), or 5% BSA in TBST for 1 hour at room temperature. Next, primary antibodies: mouse monoclonal anti-E-cadherin (E-cadherin/CDH1 Antibody, 4A2C7; Invitrogen, Carlsbad, CA) diluted 1:1000 and mouse monoclonal anti-Actin (clone C4 , Merck Millipore) diluted 1:10,000, were applied for each protein and incubated overnight at 4°C. The membranes were washed with TBST three times before incubating with the corresponding secondary anti-mouse (#G21040) IgG antibody conjugated with horseradish peroxidase (Thermo Fisher Scientific) in Can Get Signal Solution 2 (TOYOBO) for 1 h at room temperature. Signals were developed with Immobilon Western Chemiluminescent HRP substrate (#WBKLS0500, Merck Millipore) and visualized in Image Quant LAS 4000 mini luminescent image analyzer (Cytiva, MA, USA). The intensities of detected bands ware analyzed by ImageJ (National Institutes of Health, Betheads, MD, USA). The results were normalized to the β-actin level.

Statistical analysis

Volcano plots were constructed, and Student's *t*-tests were performed using Excel 2016. The Mann-Whitney test was used for comparing the average DNA methylation levels between the epithelial and mesenchymal phenotypes. The chi-squared test was used for assessing statistical differences between the epithelial and mesenchymal

phenotypes for each gene with respect to the number of patients with de novo hypermethylation.

Gene ontology analysis

Gene ontology analysis was performed using DAVID [33, 34]. DAVID analyses were performed online with a count of >10 and Benjamini–Hochberg-corrected p-values < 0.05.

Table 1. Characteristics of patients

Breed	Age	Gender	Site
Chihuahua	15	M	oral
Miniature Dachshund	12	M	oral
Chihuahua	11	F	oral
Shiba	NA	M	palate
Pug	14	M	oral
Toy poodle	13	F	oral
Border Collie	10	M	oral
Shepherd	9	F	oral/tongue
Mix	15	M	oral
Labrador retriever	11	M	oral
Pomeranian	13	M	oral
Golden retriever	10	M	oral
Shi Tzu	14	M	oral
Pug	12	F	oral
Miniature Dachshund	12	F	oral
Mix	9	F	lip
Labrador retriever	13	F	palate
Miniature Dachshund	12	F	oral
Miniature Dachshund	9	M	oral
Mix	12	M	palate
Shetland sheepdog	8	M	oral
Shetland sheepdog	10	M	tonsil
Flat coated retriever	9	F	oral
Labrador retriever	12	F	tongue
Shetland sheepdog	10	M	lip
Mix	10	M	tongue
Miniature Dachshund	12	M	oral

Abbreviations: F, female; M, male; NA, not available

Results

Sample classification into epithelial phenotype and mesenchymal phonotype

For classifying malignant melanoma samples into epithelial and mesenchymal phenotypes, E-cadherin expression, which is considered the most characteristic epithelial phenotypic marker in the process of EMT, was examined in 24 samples using immunohistochemistry or western blotting (10 samples were examined using immunohistochemistry, 22 using western blotting, and 8 using both methods). E-cadherin expression was detected in 60% (6/10) of the samples via immunohistochemistry (Fig. 1). In contrast, 73% (16/22) of the samples showed moderate to strong E-cadherin expression according to western blotting (Fig. 2). The expression patterns of E-cadherin examined using both methods were consistent in 75% (6/8) of the samples. The western blotting results were prioritized for two samples presenting conflicting results with the two methods. Finally, 16 samples were classified into the epithelial phenotype and 8 into the mesenchymal phenotype.

Comparison of DNA methylation pattern between epithelial phenotype and mesenchymal phenotype

A total of 5.1–30.4 million reads were generated from all 34 samples assayed for DNA methylation. Approximately 81,000–180,000 CpG sites with more than 20 reads were selected for each sample, and the 46,673 CpG sites common across the 34 samples were used for downstream analyses. Of the 46,673 CpG sites, 18,489 were located in CGIs and 28,184 in NCGIs.

First, the average DNA methylation level was compared for determining the differences in global DNA methylation status between the epithelial and mesenchymal phenotypes. The average DNA methylation levels were calculated using all 46,673 CpG sites, that is, 18,489 sites located in CGIs, 28,184 in NCGIs, 3,089 in CGI promoters, and 1,616 in NCGI promoters. Remarkable differences were not detected between the two phenotypes with respect to the average DNA methylation levels of all CpG sites, that is, CpG sites in CGIs, NCGIs, CGI promoters, and NCGI promoters (Table.2).

Next, the average DNA methylation for each site in CGI promoters was analyzed for identifying the differentially methylated genes between epithelial and mesenchymal phenotypes owing to the correlation between DNA methylation and gene expression in EMT. Volcano plots of 3089 sites in CGI promoters revealed that the epithelial phenotype exhibited more methylated sites (2,291 sites) than the mesenchymal phenotype (798 sites) (Fig. 4). When differentially methylated CpG sites (DMCs) were tentatively defined as a

difference of more than 10% with a p-value less than 0.05, the epithelial phenotype exhibited 17 hypermethylated sites and the mesenchymal phenotype, 6 hypermethylated sites. These 23 DMCs were included in 23 genes, and several of these genes were annotated with “ECM-receptor interaction” by gene ontology analysis; however, no statistical significance was detected. Next, I focused on de novo hypermethylation, as defined in Chapter 1 and found that 12 out of 23 genes showed de novo hypermethylation. To consider the DNA methylation level of individual samples, I determined the number of patients with de novo hypermethylation of these genes in both epithelial and mesenchymal phenotypes. Two genes, *ITAGV* and *NEUROG*, were found to be significantly hypermethylated in the epithelial phenotype.

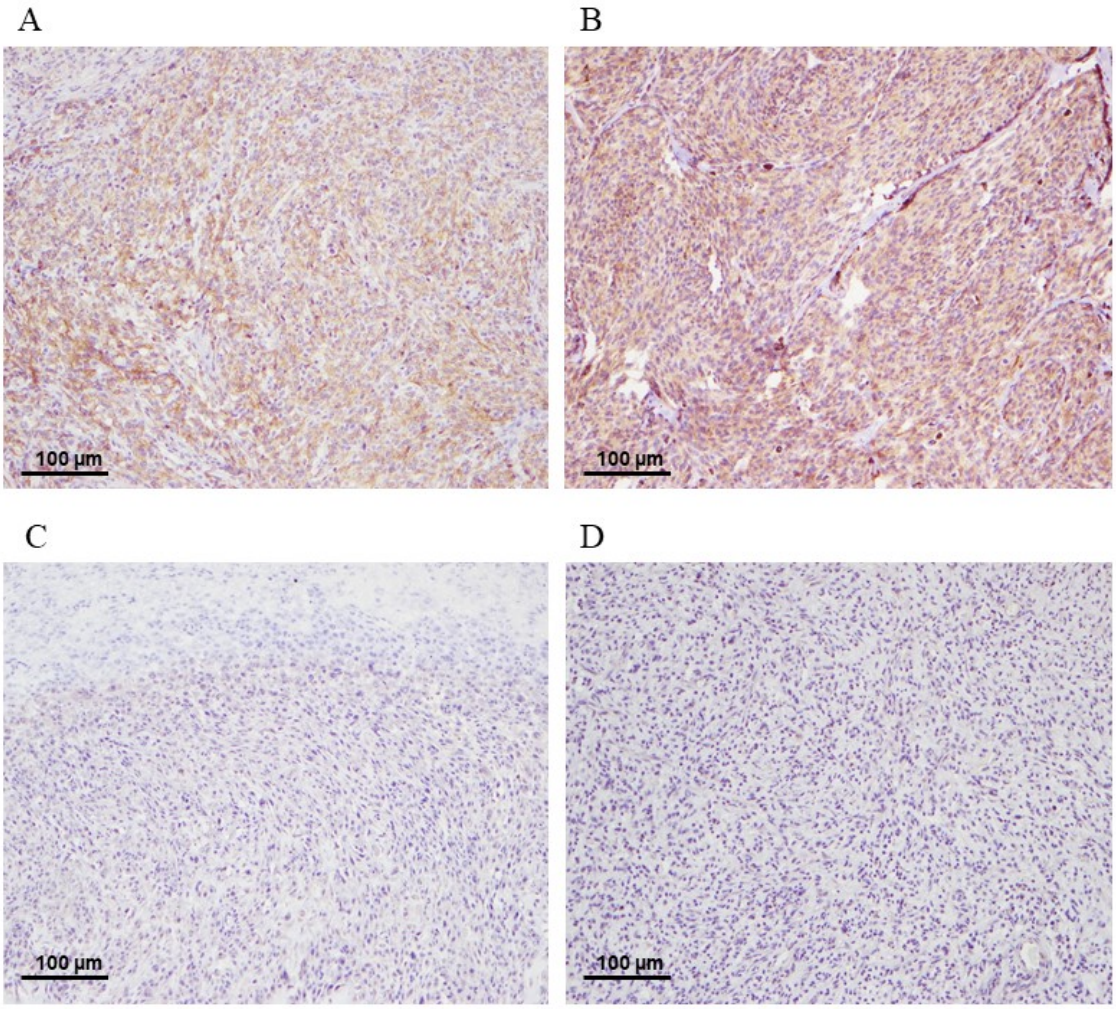

Fig.1. Immunohistochemistry for E-cadherin.

Examples of immunohistochemistry are shown for intense immunolabeling (A), (B) and low immunolabeling (C), (D).

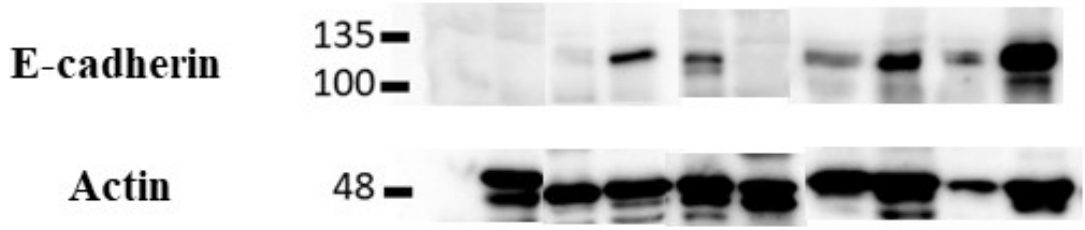

Fig.2. Western blotting for E-cadherin. Examples of western blotting are shown.

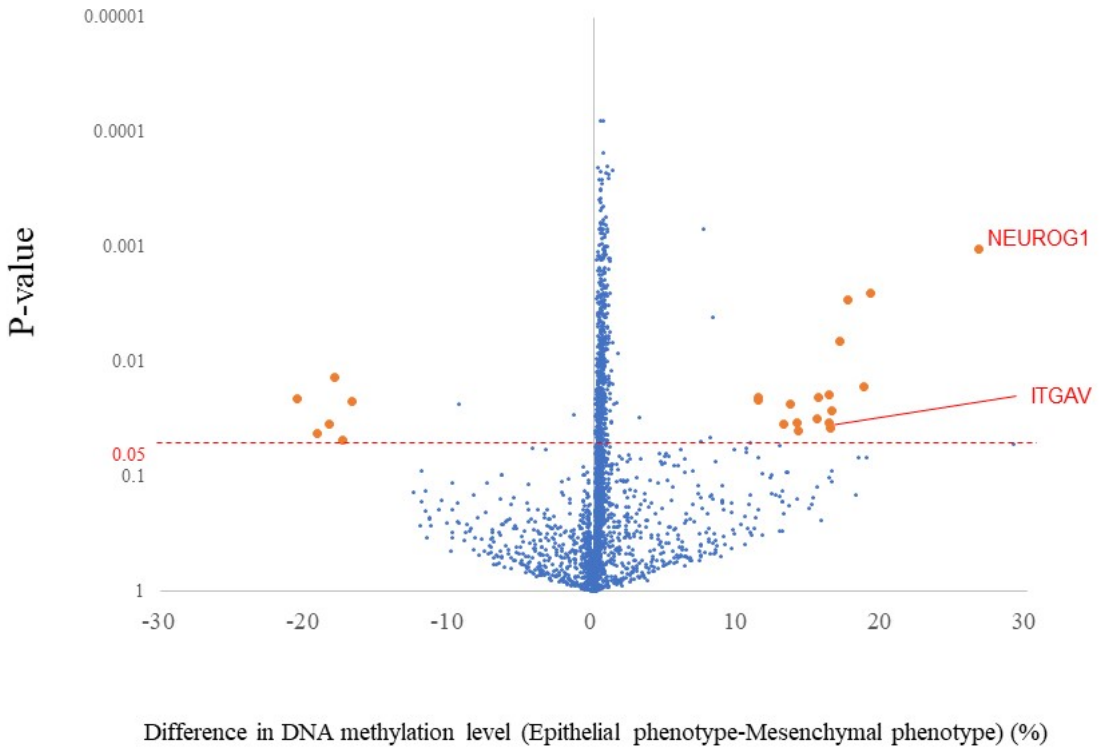

Fig.3. Difference in DNA methylation levels of Epithelial phenotype and Mesenchymal phenotype. Volcano plots with the difference in DNA methylation between average of Epithelial phenotype versus Mesenchymal phenotype on the X asis, and unajusted p-value for each site on y-axis for sites in CGI promoters. Orange dots indicate DMCs. Two genes with de novo hypermethylation are shown.

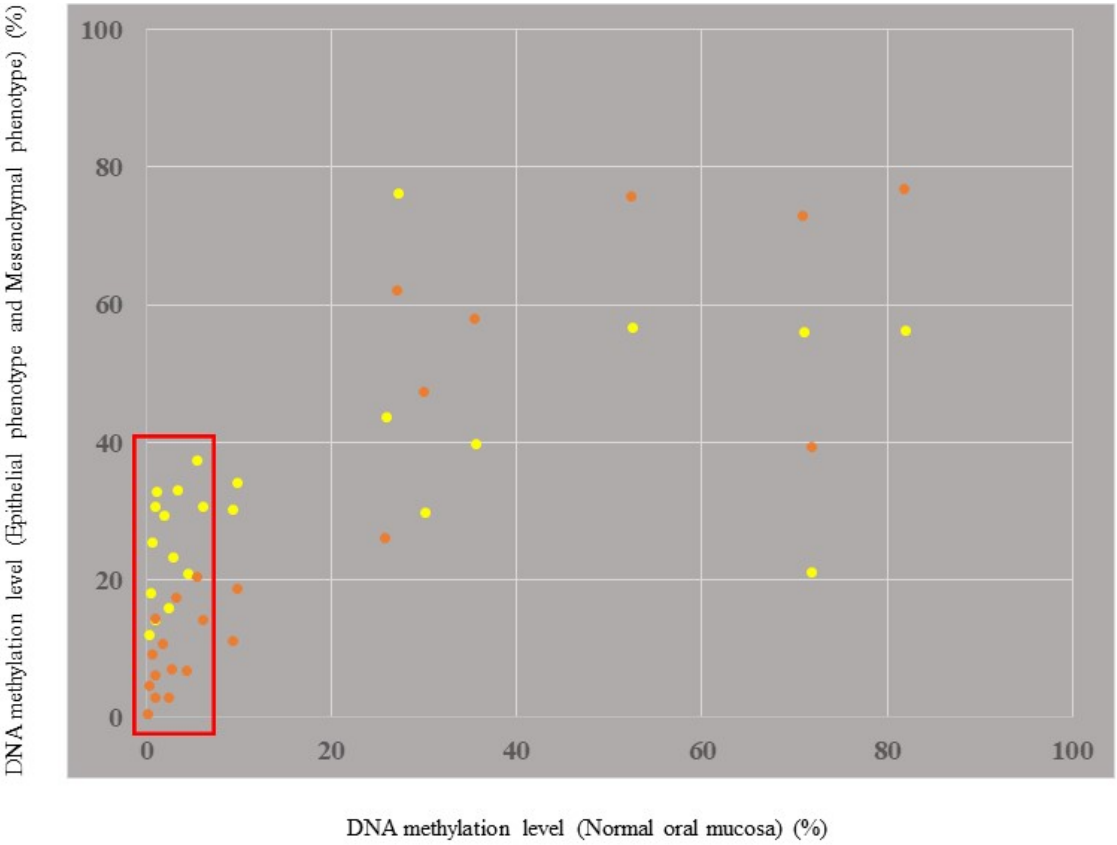

Fig.4. DNA methylation level of differentially methylated genes between two phenotypes along with normal oral mucosa. Hypermethylated genes in epithelial and mesenchymal phenotype are shown as yellow dots and orange dots respectively. De novo hypermethylated genes are within red square.

Table.2. Average DNA methylation level of each sample of epithelial phenotype and mesenchymal phenotype

	Epithelial phenotype (n=16)	Mesenchymal phenotype (n=8)	p-value
Average of DNA methylation in all site (%) : 46,673 sites	49.6	50.3	0.976
Average of DNA methylation in CGIs (%) : 18,489 sites	32.9	33.4	0.976
Average of DNA methylation in NCGIs (%) : 28,183 sites	60.6	61.4	0.976
Average of DNA methylation in CGI promoters (%) : 3,089 sites	7.8	7.3	0.209
Average of DNA methylation in NCG promoters (%) : 1,617 sites	32.7	32.4	0.69

Discussion

In this study, differences in DNA methylation patterns between epithelial and mesenchymal phenotypes in canine malignant mucosal melanoma were assessed using genome-wide DNA-methylation data analyzed using DREAM. First, the samples were classified into epithelial or mesenchymal phenotypes on the basis of E-cadherin expression. E-cadherin is a glycoprotein involved in cell-to-cell adhesion, and the loss of E-cadherin expression is the most well-known characteristic of EMT [68]. In this study, E-cadherin expression was detected in 60% of the samples by immunohistochemistry and in 73% of the samples by western blotting. These findings were relatively consistent with a previous study wherein approximately 60% of canine oral malignant melanomas showed moderate-to-marked E-cadherin expression according to immunohistochemistry [65].

Next, global DNA methylation status in both phenotypes was compared by calculating the average DNA methylation of all CpG sites, CpG sites in CGIs, NCGIs, CGI promoters, and NCGI promoters. No significant differences were detected between the two phenotypes with respect to the DNA methylation levels of all CpG sites, that is, CpG sites in CGIs, NCGIs, CGI promoters, and NCGI promoters. In a previous study of

human cutaneous malignant melanoma, the global DNA methylation level analyzed using methyl-cytosine ELISA was higher in cutaneous malignant melanoma cell lines with a proliferative phenotype (equivalent to epithelial phenotype) than in those with an invasive phenotype (equivalent to mesenchymal phenotype) [69]. This inconsistency is conceivably due to differences in the analysis methods. In this study, the global methylation status was estimated by calculating the average methylation level of limited CpG sites that were analyzed by DREAM. Therefore, it is necessary to analyze global DNA methylation levels using methylcytosine ELISA for precisely comparing the results. Furthermore, the classification of phenotypes was based on expression of the cell adhesion marker E-cadherin in the present study, whereas in a previous study, it was based on expression of the pigmentation marker MLANA. Therefore, unification of the phenotypic classification methods is necessary.

Next, when the difference in DNA methylation between the epithelial and mesenchymal phenotypes was analyzed, the epithelial phenotype exhibited 17 hypermethylated sites and 6 hypomethylated sites. Additionally, differences in DNA methylation status between epithelial and mesenchymal phenotypes have been reported in a study on human melanoma [70].

To estimate the functional relevance of differentially methylated genes, the DNA

methylation levels of these genes were assessed between the two phenotypes and for normal oral mucosa; 12 out of 23 genes showed de novo hypermethylation. When the DNA methylation level of individual samples, rather than the average DNA methylation level, was considered, the genes *ITAGV* and *NEUROG* were found to be significantly hypermethylated in the epithelial phenotype. *ITGAV* produces integrin, which functions as a cell-surface adhesion molecule and mesenchymal marker [16]. Another mesenchymal marker N-cadherin promotes neurogenin 1 expression, which is encoded by *NEUROG* [71]. Therefore, it is reasonable that both genes were methylated in the epithelial phenotype, which led to the silencing of gene expression; however, the gene expression was not evaluated in this study.

In this study, differences in the DNA methylation status between epithelial and mesenchymal phenotypes were revealed in canine mucosal malignant melanoma. Evaluation of DNA methylation can be used for assessing the effect of the demethylating agent on methylation status in tumors. Demethylating agents have been reported to reverse resistance to cancer therapy acquired via an EMT-mediated process [72]. The results from this study suggest the prospect of using demethylating agents as therapeutic agents in combination with other therapies.

Summary

EMT plays a crucial role in cancer progression by inducing enhanced migratory capacity, invasiveness, and elevated resistance to apoptosis or therapeutic agents in various neoplasia. Although epigenetic mechanisms are considered to influence EMT, there are no reports regarding the effect of DNA methylation on EMT in canine tumors.

In this chapter, we examined the differences in DNA methylation status between epithelial and mesenchymal phenotypes in canine malignant mucosal melanoma. No remarkable difference was observed in global DNA methylation status between epithelial and mesenchymal phenotypes. However, the epithelial phenotype exhibited more hypermethylated CpG sites in CGI promoters than the mesenchymal phenotype. In addition, two genes associated with cell adhesion showed de novo hypermethylation in the epithelial phenotype.

The results from this study indicate the influence of DNA methylation on EMT in canine malignant mucosal melanoma and suggest the therapeutic potential of demethylating agents in the future.

Conclusion

DNA methylation is one of the epigenetic modifications that regulate gene expression without changes in genomic sequences. DNA methylation is focused to be an important factor in many diseases including neoplasia. Global hypomethylation and specific hypermethylation in CGIs at gene promoter are specifically associated with carcinogenesis. Although there are relatively many reports for DNA methylation in canine neoplasia, studies for DNA methylation in canine malignant melanoma are still few. The goal of this study was to investigate DNA methylation status in canine malignant melanoma that is not well understood.

In chapter 1, genome-wide DNA methylation analysis in malignant melanoma cell lines and malignant melanoma clinical samples was performed by using NGS. Widespread DNA methylation alterations including hypermethylation in CGIs and hypomethylation in NCGIs were detected. These results were consistent with the findings in human cancers suggesting that changes in DNA methylation patterns are based on tumorigenic transformation. In addition, a large number of CpG sites in the CGI promoter region of genes were hypermethylated. Although the effects of aberrant DNA methylation on gene expression changes and their relevance to tumorigenesis were not assessed in this

study, these signatures of aberrant DNA methylation could be used as diagnostic or prognostic markers in canine malignant melanoma.

In chapter 2, DNA methylation status of LINE-1 in canine mucosal malignant melanoma was investigated using bisulfite-pyrosequencing which is a highly sensitive and high-throughput method to quantify CpG site methylation. LINE-1 repetitive elements are the most well recognized repetitive elements that account for about 17 % of human genome. Therefore, LINE-1 DNA methylation status is considered to represent global methylation status. In this study, malignant melanoma showed hypomethylation of LINE-1 compared to normal tissue. Furthermore, LINE-1-low patients showed worse overall survival compared with LINE-1-high patients. These results indicated that LINE-1 DNA methylation level could be used as a surrogate marker of global DNA methylation level and prognosis in canine oral malignant melanoma.

In chapter 3, difference in DNA methylation pattern between epithelial and mesenchymal phenotypes in canine malignant mucosal melanoma were assessed using genome-wide DNA methylation data analyzed by NGS. Although no remarkable difference was observed in global DNA methylation status between epithelial and mesenchymal phenotypes, the epithelial phenotype exhibited more hypermethylated CpG sites in CGI promoters than the mesenchymal phenotype. In addition, two genes

associated with cell adhesion showed de novo hypermethylation in the epithelial phenotype. The results from this study indicate the influence of DNA methylation on EMT in canine malignant mucosal melanoma and suggest the therapeutic potential of demethylating agents in the future.

In these studies, drastic DNA methylation changes in canine malignant melanoma were revealed. Although continuous studies with a greater number of clinical cases or investigation of functional effects of the observed DNA methylation changes are required, these results should contribute to elucidation of epigenetic mechanisms in canine malignant melanoma.

Acknowledgements

The author sincerely acknowledges Professor Takashi Kimura, Laboratory of Comparative Pathology, Department of Veterinary Clinical Sciences, Graduate School of Veterinary Medicine, Hokkaido University for providing the opportunity of this work and continuous guidance.

The author sincerely appreciates Professor Mitsuyoshi Takiguchi, Laboratory of Veterinary Internal Medicine, Department of Veterinary Clinical Sciences, Graduate School of Veterinary Medicine, Hokkaido University for his critical review of the manuscript and encouragement.

The author gratefully appreciates Associate Professor Jumpei Yamazaki, Graduate School of Veterinary Medicine, Veterinary Teaching Hospital, Translational Research Unit, Hokkaido University for his dedicated teaching, continuous guidance and encouragement.

The author is grateful to Associate Professor Osamu Ichii, Laboratory of Veterinary Anatomy, Graduate School of Veterinary Medicine, Hokkaido University for his cirical comment on this study.

The author really appreciates Assistant Professor Keisuke Aoshima, Laboratory

of Comparative Pathology, Department of Veterinary Clinical Sciences, Graduate School of Veterinary Medicine, Hokkaido University for providing many protocols of experiment and advises.

The author thanks all members of Laboratory of Comparative Pathology, Department of Veterinary Clinical Sciences, Graduate School of Veterinary Medicine, Hokkaido University.

The author's gratitude also goes to Dr. Yumiko Kagawa who is a supervisor of workplace North Lab (Sapporo, Japan) and all colleagues for their cooperation.

Lastly, the author would like to thank Drs. Takayuki Nakagawa (The University of Tokyo), Tsuyoshi Kadosawa (Japan Small Animal Medical Center), Kazutoshi Sakai (Rakuno Gakuen University), Hiroki Sakai (Gifu University), and Satoshi Takagi (Azabu University) for providing precious samples.

References

1. Smith SH, Goldschmidt MH, McManus PM. A comparative review of melanocytic neoplasms. Vet Pathol 2002;39(6):651-78.
2. Hendricks WPD, Zismann V, Sivaprakasam K*, et al.* Somatic inactivating PTPRJ mutations and dysregulated pathways identified in canine malignant melanoma by integrated comparative genomic analysis. PLoS Genet 2018;14(9):e1007589.
3. Palma SD, McConnell A, Verganti S*, et al.* Review on Canine Oral Melanoma: An Undervalued Authentic Genetic Model of Human Oral Melanoma? Vet Pathol 2021;58(5):881-889.
4. Gao L, Smit MA, van den Oord JJ*, et al.* Genome-wide promoter methylation analysis identifies epigenetic silencing of MAPK13 in primary cutaneous melanoma. Pigment Cell Melanoma Res 2013;26(4):542-54.
5. Lauss M, Haq R, Cirenajwis H*, et al.* Genome-Wide DNA Methylation Analysis in Melanoma Reveals the Importance of CpG Methylation in MITF Regulation. J Invest Dermatol 2015;135(7):1820-1828.
6. Razin A, Cedar H. DNA methylation and gene expression. Microbiol Rev 1991;55(3):451-8.
7. Illingworth RS, Bird AP. CpG islands--'a rough guide'. FEBS Lett 2009;583(11):1713-20.
8. Herman JG, Latif F, Weng Y*, et al.* Silencing of the VHL tumor-suppressor gene by DNA methylation in renal carcinoma. Proc Natl Acad Sci U S A 1994;91(21):9700-4.
9. Merlo A, Herman JG, Mao L*, et al.* 5' CpG island methylation is associated with transcriptional silencing of the tumour suppressor p16/CDKN2/MTS1 in human cancers. Nat Med 1995;1(7):686-92.
10. Ehrlich M. DNA hypomethylation in cancer cells. Epigenomics 2009;1(2):239-59.
11. Epiphanio TMF, Fernandes N, de Oliveira TF*, et al.* Global DNA methylation of peripheral blood leukocytes from dogs bearing multicentric non-Hodgkin lymphomas and healthy dogs: A comparative study. PLoS One 2019;14(3):e0211898.
12. Scattone NV, Epiphanio TMF, Caddrobi KG*, et al.* Quantification of Global DNA Methylation in Canine Melanotic and Amelanotic Oral Mucosal Melanomas and Peripheral Blood Leukocytes From the Same Patients With OMM: First Study. Front Vet Sci 2021;8:680181.

13. Noguchi S, Mori T, Nakagawa T*, et al.* DNA methylation contributes toward silencing of antioncogenic microRNA-203 in human and canine melanoma cells. Melanoma Res 2015;25(5):390-8.
14. Estecio MR, Gharibyan V, Shen L*, et al.* LINE-1 hypomethylation in cancer is highly variable and inversely correlated with microsatellite instability. PLoS One 2007;2(5):e399.
15. Yang AS, Estecio MR, Doshi K*, et al.* A simple method for estimating global DNA methylation using bisulfite PCR of repetitive DNA elements. Nucleic Acids Res 2004;32(3):e38.
16. Kalluri R, Weinberg RA. The basics of epithelial-mesenchymal transition. J Clin Invest 2009;119(6):1420-8.
17. Kahlert UD, Joseph JV, Kruyt FAE. EMT- and MET-related processes in nonepithelial tumors: importance for disease progression, prognosis, and therapeutic opportunities. Mol Oncol 2017;11(7):860-877.
18. Pedri D, Karras P, Landeloos E*, et al.* Epithelial-to-mesenchymal-like transition events in melanoma. FEBS J 2022;289(5):1352-1368.
19. Kiesslich T, Pichler M, Neureiter D. Epigenetic control of epithelial-mesenchymal-transition in human cancer. Mol Clin Oncol 2013;1(1):3-11.
20. Brandao YO, Toledo MB, Chequin A*, et al.* DNA Methylation Status of the Estrogen Receptor alpha Gene in Canine Mammary Tumors. Vet Pathol 2018;55(4):510-516.
21. Tomiyasu H, Fujiwara-Igarashi A, Goto-Koshino Y*, et al.* Evaluation of DNA methylation profiles of the CpG island of the ABCB1 gene in dogs with lymphoma. Am J Vet Res 2014;75(9):835-41.
22. Yamazaki J, Jelinek J, Hisamoto S*, et al.* Dynamic changes in DNA methylation patterns in canine lymphoma cell lines demonstrated by genome-wide quantitative DNA methylation analysis. Vet J 2018;231:48-54.
23. Inoue K, Ohashi E, Kadosawa T*, et al.* Establishment and characterization of four canine melanoma cell lines. J Vet Med Sci 2004;66(11):1437-40.
24. Ohashi E, Hong SH, Takahashi T*, et al.* Effect of retinoids on growth inhibition of two canine melanoma cell lines. J Vet Med Sci 2001;63(1):83-6.
25. Lee BH, Neela PH, Kent MS*, et al.* IQGAP1 is an oncogenic target in canine melanoma. PLoS One 2017;12(4):e0176370.
26. Ushio N, Rahman MM, Maemura T*, et al.* Identification of dysregulated microRNAs in canine malignant melanoma. Oncol Lett 2019;17(1):1080-1088.
27. Jelinek J, Liang S, Lu Y*, et al.* Conserved DNA methylation patterns in healthy

blood cells and extensive changes in leukemia measured by a new quantitative technique. Epigenetics 2012;7(12):1368–1378.
28. Gardiner-Garden M, Frommer M. CpG islands in vertebrate genomes. J Mol Biol 1987;196(2):261-82.
29. Guo H, Zhu P, Yan L*, et al.* The DNA methylation landscape of human early embryos. Nature 2014;511(7511):606-10.
30. Vorjohann S, Pitetti JL, Nef S*, et al.* DNA methylation profiling of the fibrinogen gene landscape in human cells and during mouse and zebrafish development. PLoS One 2013;8(8):e73089.
31. Crider KS, Yang TP, Berry RJ*, et al.* Folate and DNA methylation: a review of molecular mechanisms and the evidence for folate's role. Adv Nutr 2012;3(1):21-38.
32. Lund K, Cole JJ, VanderKraats ND*, et al.* DNMT inhibitors reverse a specific signature of aberrant promoter DNA methylation and associated gene silencing in AML. Genome Biol 2014;15(8):406.
33. Huang da W, Sherman BT, Lempicki RA. Bioinformatics enrichment tools: paths toward the comprehensive functional analysis of large gene lists. Nucleic Acids Res 2009;37(1):1-13.
34. Huang DW, Sherman BT, Lempicki RA. Systematic and integrative analysis of large gene lists using DAVID bioinformatics resources. Nature Protocols 2009;4(1):44-57.
35. Jones PA, Baylin SB. The epigenomics of cancer. Cell 2007;128(4):683-92.
36. Byun HM, Siegmund KD, Pan F*, et al.* Epigenetic profiling of somatic tissues from human autopsy specimens identifies tissue- and individual-specific DNA methylation patterns. Hum Mol Genet 2009;18(24):4808-17.
37. Taby R, Issa JP. Cancer epigenetics. CA Cancer J Clin 2010;60(6):376-92.
38. Li JL, Mazar J, Zhong C*, et al.* Genome-wide methylated CpG island profiles of melanoma cells reveal a melanoma coregulation network. Sci Rep 2013;3:2962.
39. Mark M, Rijli FM, Chambon P. Homeobox genes in embryogenesis and pathogenesis. Pediatr Res 1997;42(4):421-9.
40. Schlesinger Y, Straussman R, Keshet I*, et al.* Polycomb-mediated methylation on Lys27 of histone H3 pre-marks genes for de novo methylation in cancer. Nat Genet 2007;39(2):232-6.
41. Widschwendter M, Fiegl H, Egle D*, et al.* Epigenetic stem cell signature in cancer. Nat Genet 2007;39(2):157-8.
42. Shah N, Sukumar S. The Hox genes and their roles in oncogenesis. Nat Rev Cancer 2010;10(5):361-71.

43. Bork S, Pfister S, Witt H, *et al.* DNA methylation pattern changes upon long-term culture and aging of human mesenchymal stromal cells. Aging Cell 2010;9(1):54-63.
44. Noushmehr H, Weisenberger DJ, Diefes K, *et al.* Identification of a CpG island methylator phenotype that defines a distinct subgroup of glioma. Cancer Cell 2010;17(5):510-22.
45. Toyota M, Kopecky KJ, Toyota MO, *et al.* Methylation profiling in acute myeloid leukemia. Blood 2001;97(9):2823-9.
46. Toyota M, Ahuja N, Ohe-Toyota M, *et al.* CpG island methylator phenotype in colorectal cancer. Proc Natl Acad Sci U S A 1999;96(15):8681-6.
47. Tanemura A, Terando AM, Sim MS, *et al.* CpG island methylator phenotype predicts progression of malignant melanoma. Clin Cancer Res 2009;15(5):1801-7.
48. Lee JH, Miele ME, Hicks DJ, *et al.* KiSS-1, a novel human malignant melanoma metastasis-suppressor gene. J Natl Cancer Inst 1996;88(23):1731-7.
49. Ji K, Ye L, Mason MD, *et al.* The Kiss-1/Kiss-1R complex as a negative regulator of cell motility and cancer metastasis (Review). Int J Mol Med 2013;32(4):747-54.
50. Keshet I, Schlesinger Y, Farkash S, *et al.* Evidence for an instructive mechanism of de novo methylation in cancer cells. Nat Genet 2006;38(2):149-53.
51. Eden A, Gaudet F, Waghmare A, *et al.* Chromosomal instability and tumors promoted by DNA hypomethylation. Science 2003;300(5618):455.
52. Inamura K, Yamauchi M, Nishihara R, *et al.* Tumor LINE-1 methylation level and microsatellite instability in relation to colorectal cancer prognosis. J Natl Cancer Inst 2014;106(9).
53. Pattamadilok J, Huapai N, Rattanatanyong P, *et al.* LINE-1 hypomethylation level as a potential prognostic factor for epithelial ovarian cancer. Int J Gynecol Cancer 2008;18(4):711-7.
54. Sigalotti L, Fratta E, Bidoli E, *et al.* Methylation levels of the "long interspersed nucleotide element-1" repetitive sequences predict survival of melanoma patients. J Transl Med 2011;9:78.
55. Aparicio A, North B, Barske L, *et al.* LINE-1 methylation in plasma DNA as a biomarker of activity of DNA methylation inhibitors in patients with solid tumors. Epigenetics 2009;4(3):176-84.
56. Karami S, Andreotti G, Liao LM, *et al.* LINE1 methylation levels in pre-diagnostic leukocyte DNA and future renal cell carcinoma risk. Epigenetics 2015;10(4):282-92.
57. Lee KH, Shin TJ, Kim WH, *et al.* Methylation of LINE-1 in cell-free DNA serves

as a liquid biopsy biomarker for human breast cancers and dog mammary tumors. Sci Rep 2019;9(1):175.
58. Colella S, Shen L, Baggerly KA*, et al.* Sensitive and quantitative universal Pyrosequencing methylation analysis of CpG sites. Biotechniques 2003;35(1):146-50.
59. Jurka J, Kapitonov VV, Pavlicek A*, et al.* Repbase Update, a database of eukaryotic repetitive elements. Cytogenet Genome Res 2005;110(1-4):462-7.
60. Gaudet F, Hodgson JG, Eden A*, et al.* Induction of tumors in mice by genomic hypomethylation. Science 2003;300(5618):489-92.
61. Smedley RC, Spangler WL, Esplin DG*, et al.* Prognostic markers for canine melanocytic neoplasms: a comparative review of the literature and goals for future investigation. Vet Pathol 2011;48(1):54-72.
62. Kosumi K, Baba Y, Okadome K*, et al.* Tumor Long-interspersed Nucleotide Element-1 Methylation Level and Immune Response to Esophageal Cancer. Ann Surg 2019; 10.1097/SLA.0000000000003264.
63. Nosho K, Baba Y, Tanaka N*, et al.* Tumour-infiltrating T-cell subsets, molecular changes in colorectal cancer, and prognosis: cohort study and literature review. J Pathol 2010;222(4):350-66.
64. Moustakas A, Heldin CH. Signaling networks guiding epithelial-mesenchymal transitions during embryogenesis and cancer progression. Cancer Sci 2007;98(10):1512-20.
65. Silvestri S, Porcellato I, Mechelli L*, et al.* E-Cadherin Expression in Canine Melanocytic Tumors: Histological, Immunohistochemical, and Survival Analysis. Vet Pathol 2020;57(5):608-619.
66. Veloso ES, Goncalves INN, Silveira TL*, et al.* ZEB and Snail expression indicates epithelial-mesenchymal transition in canine melanoma. Res Vet Sci 2020;131:7-14.
67. Urbanova M, Buocikova V, Trnkova L*, et al.* DNA Methylation Mediates EMT Gene Expression in Human Pancreatic Ductal Adenocarcinoma Cell Lines. Int J Mol Sci 2022;23(4).
68. Fonseca-Alves CE, Kobayashi PE, Leis-Filho AF*, et al.* E-Cadherin Downregulation is Mediated by Promoter Methylation in Canine Prostate Cancer. Front Genet 2019;10:1242.
69. Cheng PF, Shakhova O, Widmer DS*, et al.* Methylation-dependent SOX9 expression mediates invasion in human melanoma cells and is a negative prognostic factor in advanced melanoma. Genome Biol 2015;16:42.
70. Motwani J, Rodger EJ, Stockwell PA*, et al.* Genome-wide DNA methylation and

RNA expression differences correlate with invasiveness in melanoma cell lines. Epigenomics 2021;13(8):577-598.
71. Chen J, Zacharek A, Li Y, *et al.* N-cadherin mediates nitric oxide-induced neurogenesis in young and retired breeder neurospheres. Neuroscience 2006;140(2):377-88.
72. Galle E, Thienpont B, Cappuyns S, *et al.* DNA methylation-driven EMT is a common mechanism of resistance to various therapeutic agents in cancer. Clin Epigenetics 2020;12(1):27.

Summary in Japanese

犬の悪性黒色腫は口腔内に好発し、臨床的あるいは病理学的な観点から、治療法や予後因子について多くの研究がなされている。しかし、早期診断の難しさや臨床的挙動の悪さから、治療効果は低く、致死率が非常に高い疾患である。近年、医学領域においては、遺伝子配列の変化を伴わずに表現型の変化をもたらすエピジェネティクスが着目され、悪性黒色腫を含めた腫瘍性疾患においてもエピジェネティックなメカニズムについての研究が行われている。エピジェネティック修飾の１つである DNA メチル化は、ゲノム DNA の CpG ジヌクレオチドにおけるシトシンのメチル基付加修飾で、遺伝子のプロモーター領域で起こると遺伝子発現が抑制されることが知られている。通常 CpG サイトはゲノム上に散在しているが、CpG アイランド（CGI）と呼ばれる CpG サイトが密集する領域が多くの遺伝子のプロモーター領域に存在している。腫瘍組織では CGI の一部でメチル化が増加し、NCGI の一部でメチル化が減少することが知られている。犬の悪性黒色腫の DNA メチル化に関する報告は少なく、その異常については不明な点が多い。そこで本研究では、犬の悪性黒色腫における DNA メチル化の変化を明らかにすることを目的とした。

第１章では、犬の悪性黒色腫の細胞株と臨床サンプルを用い、ゲノム上

の認識部位（CCCGGG）は同じであるが、DNA メチル化の状態によって切断形式が異なる２種類の制限酵素と次世代シークエンサーを利用して（DREAM 法）、DNA メチル化のゲノムワイド解析を行った。その結果、CGI に存在する CpG サイトの多くにメチル化の増加がみられ、また NCGI に存在する CpG サイトの多くにはメチル化の減少が認められた。更に、これら高メチル化 CpG サイトの近傍には多くの遺伝子が確認された。以上の結果から、人の腫瘍での報告と同様に、犬の悪性黒色腫においても広範囲で DNA メチル化の変化が起こっていることがわかった。

第２章では、DNA メチル化の局所解析では再現性・定量性が高いパイロシーケンス法を用い、犬の口腔内の悪性黒色腫における LINE-1 のメチル化の定量を行った。LINE-1 とはタンパク質非コード反復配列で、人のゲノムの約１７％を占めている。そのため、LINE-1 のメチル化の状態はゲノム全体のメチル化の状態を反映するとされている。LINE-1 は正常組織ではメチル化しているが、腫瘍組織では脱メチル化がおこり、活性化することでゲノムの不安定性を引き起こすとされ、LINE-1 の脱メチル化と生存期間の短さの関係性が報告されている。今回の研究では、悪性黒色腫の LINE-1 のメチル化レベルは正常組織と比較して低値であった。また、LINE-1 のメチル化が低い症例に、生存期間が短い症例が多いことが明らかとなった。以上の結果より、犬の口腔内悪性黒色腫における

LINE-1 のメチル化の状態ならびに LINE-1 のメチル化の状態と予後との相関性は、人の腫瘍での報告と一致していることがわかった。

第３章では、多くの腫瘍で報告されている可逆性プロセスである上皮間葉転換（EMT）と DNA メチル化の関連について着目した。上皮系マーカーの指標とされている E-カドヘリンの発現によって犬の悪性黒色腫を上皮系フェノタイプと間葉系フェノタイプに分類し、第１章と同じ DREAM 法を利用して得られた DNA メチル化のデータを用いて、上皮系フェノタイプと間葉系フェノタイプのメチル化状態の違いを解析した。上皮系フェノタイプでより多くの高メチル化部位が確認され、新規の高メチル化を示す２つの遺伝子が細胞間接着性因子に関連していることが明らかとなった。この結果は、犬の悪性黒色腫における EMT に DNA メチル化が関連していることを示唆するものであった。

本研究の知見は、犬の悪性黒色腫における DNA メチル化の変化の解明に寄与するものであり、今後腫瘍発生における機能的関連性の解明や予後予測、治療法の確立などに資することが期待される。